Investigations on 2,7-diamino-9-fluorenol photochemistry

INAUGURALDISSERTATION

zur
Erlangung der Würde eines Doktors der Philosophie
vorgelegt der
Philosophisch-Naturwissenschaftlichen Fakultät
der
Universität Basel

von

DRAGANA ZIVKOVIC

aus Pirot, Serbien

Basel, 2007

Genehmigt von der Philosophisch-Naturwissenschaftlichen Fakultät auf Antrag von Prof. Dr. J. Wirz und Prof. Dr. H. Huber.

Basel, den 24. 04. 2007.

Prof. Dr. Hans Peter Hauri

Dekan

Dedicated to my family

and to Ian

Acknowledgments

First of all, I would like to thank Prof. Dr. Jakob Wirz for giving me the opportunity to join his research group, for guiding and supporting my work.

I thank Prof. Dr. Hanspeter Huber for agreeing to act as co-referee.
I thank Prof. Dr. Martin Jungen for agreeing to act as chairman of the thesis committee.

A special thanks to the members of the Wirz group:
Hassen Boudebous, Martin Gaplovsky, Yavor Kamdzhilov, Gaby Persy, Bruno Hellrung, Jürgen Wintner, Pavel Müller and Dominik Heger. Thanks for making the atmosphere in the lab so enjoyable, for the useful discussions and for always being ready to help.

I thank my family and friends, especially Mat and Janni, for their affection and constant encouragement.

I thank piggy, for being there for me, and for cheering me up when experiments didn't work.

Finally, I would also like to thank the Swiss National Science Foundation and the University of Basel for their financial support.

Table of Contents

1. Introduction

Protecting groups have been long known as useful synthetic tools, especially in multistep organic synthesis. They are introduced into a molecule by chemical modification of a functional group to obtain maximum control and selectivity in the subsequent reaction. There are numerous considerations which define how effectively a protecting group will fulfill its assigned role of shielding a functional group from destruction[1,2]. The protecting group should be easily and efficiently introduced, as well as cheap and readily available. It should be stable to the widest possible range of reaction conditions and removed selectively and efficiently under highly specific conditions, leaving intact all the other groups (the so-called "orthogonality")[3]. The removal of the protecting group can be achieved by chemical, electrolytic or photolytic methods. When it is achieved photolytically, *i.e.* no reagent for its cleavage is required - just light, we are talking about photoremovable protecting groups. This category of protecting groups offers the possibility of dealing with extremely sensitive molecules, otherwise incompatible with acids or bases[4]. Also, the release of the substrate can be strictly controlled, both the concentration and the spatial distribution. Very good general reviews have been published in this field[2,5-8].

Photoremovable protecting groups are used for a broad range of applications in organic synthesis, biophysics and biology. They are commonly linked to a substrate of interest to make them unable to react, forming in this manner a "caged compound"[6-11]. The term "caged compound" was coined in 1978 for photolabile derivatives of natural substrates such as ATP, first reported by Kaplan, Forbush and Hoffman[12]. More recently, the term phototrigger has become more broadly accepted as a more accurate of the photoactive protective group. Caged compounds are widely used to start biological reactions by the photolytic release of an effector molecule from a biologically inactive precursor. Upon irradiation, typically breaking the photolabile bond with a pulse of intense light in the near ultraviolet (UV; 350–360 nm) range, the protecting group undergoes a photochemical reaction that results in release of the substrate and restores its activity. In this fashion it is possible to deliver bioactive materials such as neurotransmitters, ATP, L-glutamate, γ-aminobutyric acid (GABA) or Ca^{2+} ions

rapidly to small target sites and therefore enable following ensuing physiological events in real time. Amplified chemical effects may be achieved by controlling enzyme activity, gene expression or ion channel permeability with light (phototriggers). Typical procedure for caging and uncaging the protein is shown as an example below:

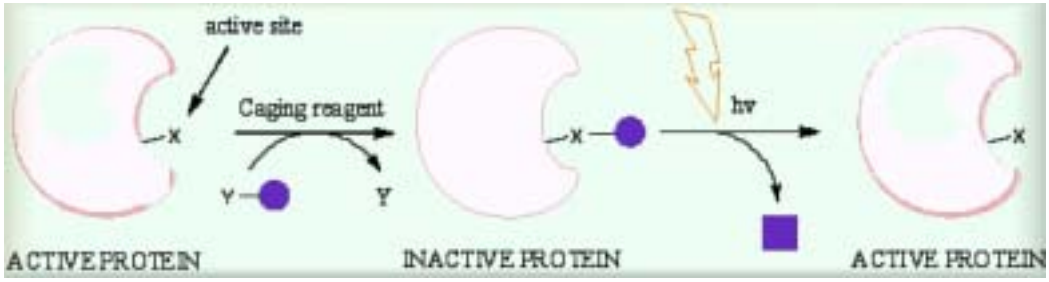

Several potential chromophores have been examined for cage applications, but only very few have met the demands or been successfully developed. The constraints include both mechanistic requirements and changes in physical properties that accompany the attachment of a chromophore to a substrate. An important limiting factor is an ease of synthesis of the substrate-cage complex; the organic synthesis is often very challenging, thus limiting selection to the cages which are commercially available.

A good photoremovable protecting group should ideally posses some or all of the properties mentioned below:

- The photoprotected substrate must be soluble in aqueous buffered media and it may be required that they can pass biological barriers such as cell membranes.
- The phototrigger must be stable to hydrolysis, especially at high ionic strengths.
- The photoreaction should be clean and efficient, *i.e.*, occur with high quantum yield $\Phi > 0.1$.
- The chromophore should have high absorptivity at wavelengths greater than 310 nm, where irradiation is less likely to be absorbed and possibly be causing damage to the biological tissue.
- The photoproduct(s) of the protecting group must be biologically benign, *i.e.*, should not affect the system investigated. Formation of the free radicals should be avoided. Also, the photochemical by-products should not interfere with the photoreaction and

ideally be transparent at the irradiation wavelength in order to avoid a light filtering effect by the product at high conversions.

- The photorelease reaction should be a primary photochemical step, *i.e.*, direct bond cleavage to the substrate from the reactive excited state, thus avoiding any long-lived intermediates prior to release of the substrate.

These criteria seldom are met in their entirety, but they do serve as guidelines for the design and development of new phototriggers. Efficient and fast systems for poor leaving groups such as RO^-, RHN^- or RS^- are sought in particular.
So far, the four photoremovable protecting groups (ppg's) that are best satisfying these requirements are: (a) 2-nitrobenzyl (2-NB), (b) benzoin (Bnz), (c) p-hydroxyphenacyl (pHP) and (d) arylmethyl derivatives including the benzyl (Bz) and coumaryl (Cou) chromophores. A summary of those ppg's with the photorelease mechanisms and selection of applications is given in the rest of this chapter.

1.1. Major photoremovable protecting groups

1.1.1. The 2-nitrobenzyl group

2-Nitrobenzyl cages (2-NB) are the first applied[12] and most widely used ppg's, in fact more than 80% of the publications on caged compounds are applications of the 2-NB chromophore and its derivatives. Still, 2-NB is by no means the most suitable ppg to apply in biology and related fields due to a number of drawbacks. Its rate of release depends on many factors, and is the slowest around physiological pH values; the final product contains a nitroso group which makes it quite reactive and toxic to living cells; at the same time, the spectrum of the photoproduct is bathochromically shifted and competes for the incident light, leading to inefficient photolysis; the absorbance of non-substituted 2-NB's is about 350 nm, therefore harmful UV irradiation cannot be avoided upon the deprotection; the release of the substrate proceeds via a complex and slow sequence of reactions, allowing trapping agents to intercept intermediates therefore retarding the release (Scheme 1).

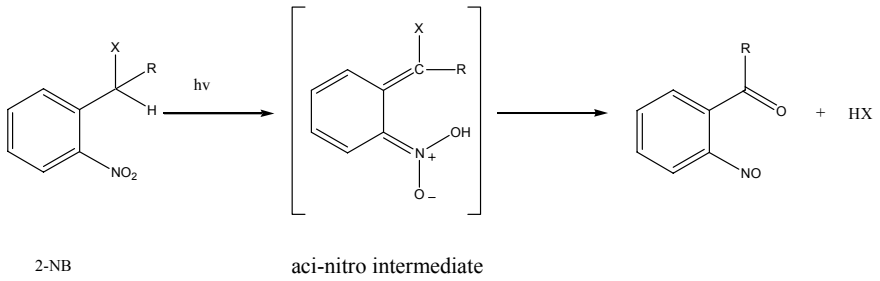

Scheme 1. Photoelimination of the substrate from the 2-nitrobenzyl group.

The events occurring between the absorption of light by the 2-NB chromophore and emergence of the unfettered substrate **HX** are shown in detail at the Scheme 2.

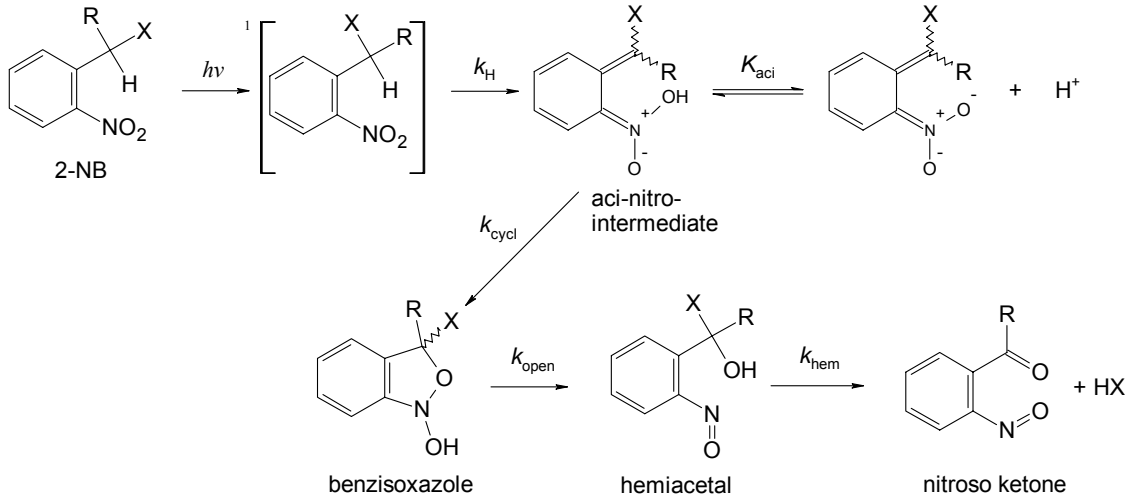

Scheme 2. Reaction mechanism of the 2-nitrobenzyl group.

This sequence depends on many factors, such as the nucleofugacity of **X**, the nature of the substituent **R**, pH and solvent. When a photon is absorbed, 2-NB is excited to its singlet state where it can either cross over to a triplet excited state or undergo a hydrogen abstraction (k_H). The multiplicity of the reactive state has not been established for all members of the NB family. It is generally accepted that hydrogen abstraction is fast enough to compete with the intersystem crossing. This shift of a proton to the oxygen leads to formation of an aci-nitro

intermediate. Wirz *et al.* [13] have shown that the *E,E*-aci nitro isomer cyclyses directly to benzisoxazole, which is a UV-VIS silent intermediate and its presence was mainly established by time-resolved IR spectroscopy. The decay of benzioxasole gives rise to new sygnals in the IR spectrum, which were assigned to hemiacetal. Its IR spectrum exhibits a strong nitroso absorption band but no sygnal for a carbonyl group. Finally, the carbonyl group stretching vibration appearance of the nitrozobenzaldehyde signals the release rate of the substrate **X**. This seems to be the only reliable measure for the release rates of the members of the 2-NB family.

1.1.2. The benzoin group

The benzoin or desyl protecting group (Desyl, Bnz) has several advantages. The chromophore strongly absorbs in the near UV region allowing for more efficient irradiation and therefore high quantum yields; its synthesis is straightforward and usually of high yield; the photoreaction is relatively clean and uniform and leads to biologically inert by-product. The overall photoreaction is shown in Scheme 3.

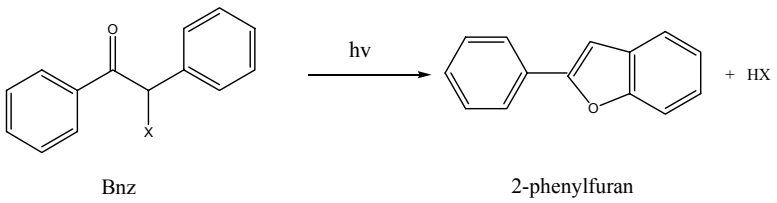

Scheme 3. Photoreaction of the benzoin group.

Several different mechanisms of release have been proposed. Wirz and Givens[14] provided sufficient information on the mechanism of the non-substituted benzoin group. They have reported two different pathways necessary to account for their results (Scheme 4).

Two competing reaction pathways (a, b) originate from the lowest triplet, established to be the reactive excited state, and are solvent dependent. In all solvents, except water and fluorinated alcohols, 2-phenylbenzofuran is formed within 20 ns, presumably via a biradical intermediate (a), which however has not been observed. It is assumed that it reacts faster than it is formed.

The second reaction pathway (b) leads to products of nucleophilic substitution and decreases the chemical yield of 2-phenylbenzofuran. A transient, observed in nanosecond LFP (λ_{max} = 570 nm, τ = 660 ns), was assigned to the triplet cation formed after loss of the leaving group. Its presence was additionally confirmed by DFT calculations and quenching studies. As the addition of nucleophiles to a triplet cation is a spin forbidden process, intersystem crossing was invoked as the next step to explain the slow addition of solvent. The partitioning of the photoreaction the authors explained with the coexistence of two interconvertible conformers of the benzoin phosphate in the ground state. The gauche conformation is disfavoured by solvents which form strong hydrogen bonds to the carbonyl group and leads to the benzofuran. The anti isomer instead is favoured by protic solvents and heterolysis generates an extended benzyl cation which leads the reaction towards nucleophilic addition.

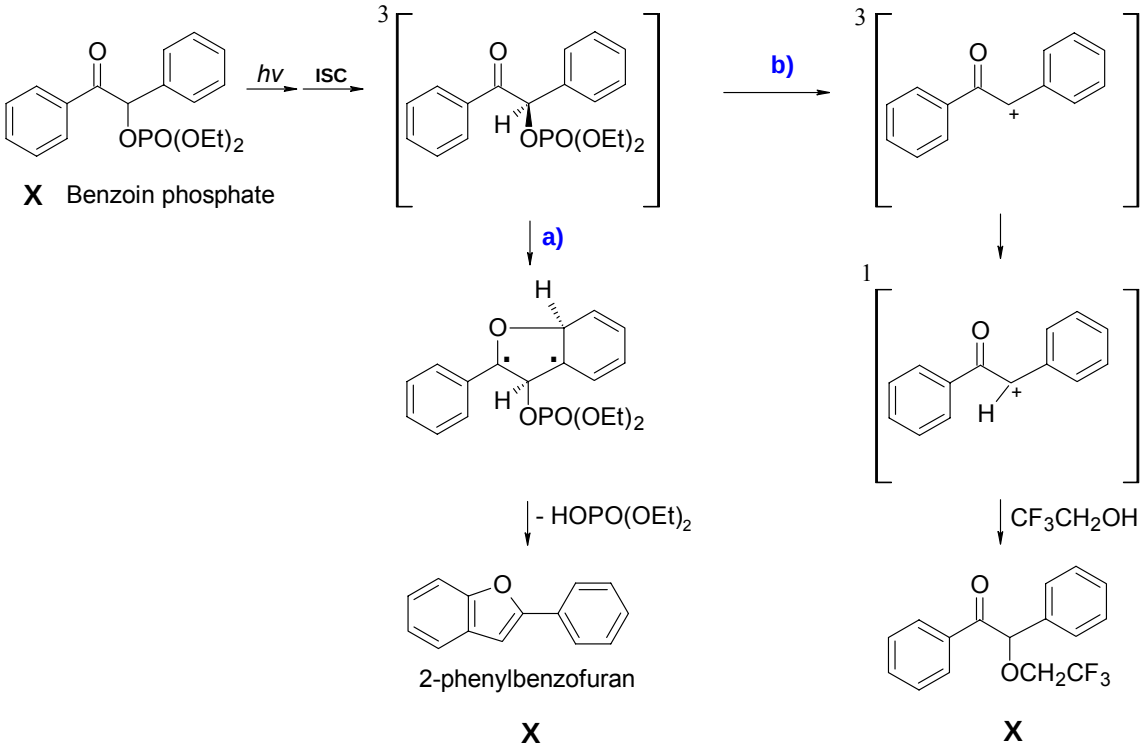

Scheme 4. Mechanism of deprotection of the non-substituted benzoin group.

Benzoin group offer a few practical applications but there are also several major drawbacks. The benzylic carbon introduces the additional chiral center which imposes a problem when optically active substrates are protected. Also, the by-product benzofuran absorbs light and acts as an internal light filter. The poor solubility of benzoin caged compounds in aqueous media acts as a limiting factor for their biological applications, but it has been solved recently by development of a water soluble benzoin cage.

1.1.3. The p-hydroxyphenacyl group

The discovery and development of the p-hydroxyphenacyl (pHP) chromophore began in the mid 1990s and continues today. It was introduced by Givens *et al.*[15] as an excellent alternative to the 2-nitrobenzyl and the benzoin groups. Its remarkable properties include fast release rates on the order of 1 ns, depending on the substrate released; high quantum yields of release; adequate solubility in aqueous media; the main by-product is transparent at the irradiation wavelength due to the blue-shift of its absorption allowing quantative chemical conversion; it is also biologically benign. However, because of its recent entry into this research area, the number of applications so far is limited but there are very informative cases of its use showing a lot of potential[16-19].

The details of the mechanism of release from pHP are still to be clarified, but there are hypothesae based on a number of photochemical studies (Scheme 5).

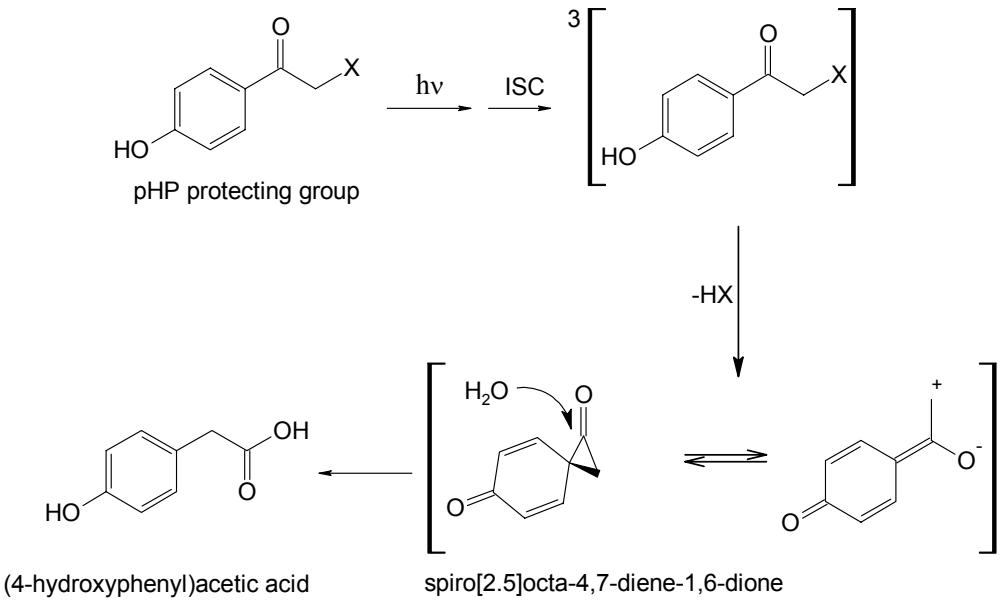

Scheme 5. Mechanism of release of pHP protecting group.

Givens *et al.*[17] reported that the reaction is quenched by naphthalene-2-sulfonate and potassium sorbate, revealing that the reaction proceeds via triplet excited state with a lifetime of 0.5 ns. Later, Wirz *et al.*[20] investigated pHP diethyl phosphate and observed the triplet excited state by pump-probe spectroscopy (λ_{max} = 380 nm, τ = 0.4 ns in acetonitrile / water = 1:1), quenchable by oxygen and piperylene. The agreement between the results has led to the conclusion that pHP expels the caged substrate from its triplet excited state even though the actual release has not been measured. The deprotection occurs either simultaneously or follows deprotonation of the para-hydroxyl group in the triplet excited state. The triplet pKa of this chromophore was measured to be 3.6 versus 7.9 in the ground state.

A major drawback of the pHP group is its weak extinction in the near UV of the spectrum and Conrad and Givens[21] had attempted to address this by synthesizing 3,5-methoxy derivative. They managed to shift favourably the absorption maximum but the quantum yield of release dropped significantly.

1.1.4. The coumarinyl group

The coumarinyl derivatives show fast rates of photorelease and are useful for 2-photon excitation. They have been applied to a number of biological studies, including the photorelease of phosphates[22], cyclic nucleotides[23-25] and carboxylic acids[22].

Schade *et al.* [22]proposed a mechanistic scheme (photo S_N1 mechanism) that outlines the photoreaction of the coumarinyl group (Scheme 6).

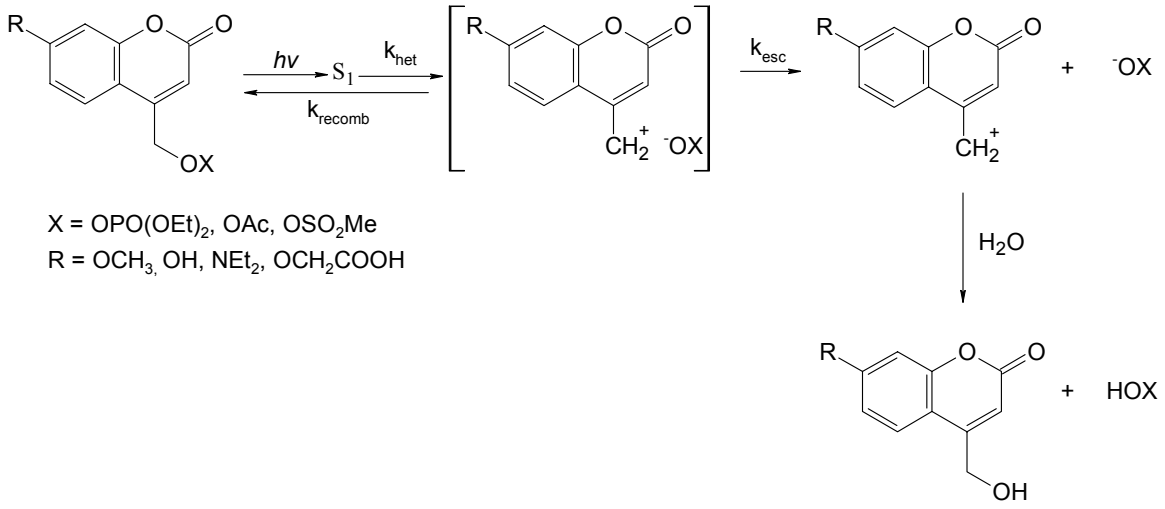

Scheme 6. Mechanism of release of the coumarinyl protecting group.

Upon the initial excitation the coumarinyl chromophore is promoted to its singlet excited state. Almost all derivatives from that series have very weak fluorescence suggesting an efficient photoreaction. The product of photolysis is on the other hand a strongly fluoerscing compound. This fact can be used to monitor the process of release. Heterolytic C-O fragmentation (k_{het}) occurs from the singlet excited state, which is most likely the rate-determining step of release ($k_{het} \sim 10^9$ s^{-1}). The absence of evidence on the initial cleaving step prevents an unequivocal classification of heterolytic versus homolytic cleavage[22,26]. Schade has shown that there is a correlation between the quantum efficiency and the polarity of the solvent. The more polar the solvent, the better the solvation of the ion pair and thus higher quantum yields.

This system has fewer drawbacks. The quantum yields of most of the derivatives are low to moderate and some of them are not stable for long times in neutral aqueous media. Still, the

high extinction coefficients in the visible range of the spectrum, the fast rate of release and the high photochemical stability of the photoproduct make the coumarinyl group a very promising one.

1.1.5. The other groups

Besides these four widely used classes of photoremovable protecting groups, there is still a number of other ppg's known and which have started to be used recently.

7-nitroindolines have been known for quite a long time but only recently have they gained attention as ppg's. Photocleavage involves the triplet excited state and proceeds in the submicrosecond range, as shown in the Scheme 7. The photoreaction is clean and strongly depends on the solvent[11].

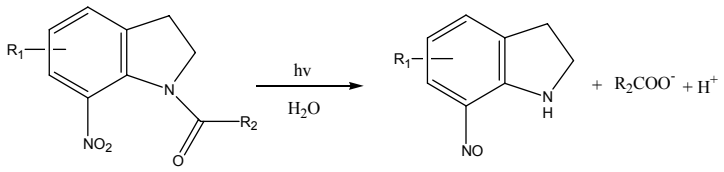

Scheme 7. Photolysis of 7-nitroindoline protecting group.

The dimethoxy benzyl group is a good protecting group for amino acids[11]. The photoreaction proceeds via short-lived excited state (Scheme 8) with the fragmentation rate constant in order of 10^8 s^{-1}. This ppg has restriction of low quantum yield.

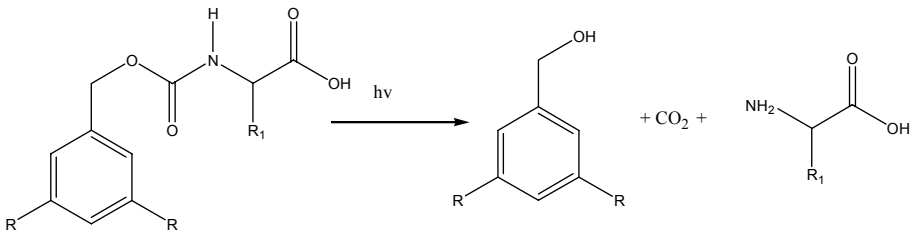

Scheme 8. Photolysis of the benzyl protecting group.

New chromophores with enhanced properties such as nitrodibenzofurane[27,28] based on the well-established 2-nitrobenzyl protecting group and 8-bromo-7-hydroxyquinoline[29,30] based on the coumarinyl ppg photochemistry are also introduced.
A comparative analysis presented here confirms that despite the high number of synthesized molecules properties of the existing photoremovable protecting groups are often not optimal and there is still need for more powerful ones. The design of new photoremovable groups is a challenging task and efficient systems are especially needed for poor leaving groups. Finding these is a secondary aim of this project.

1.2. Applications of the photoremovable protecting groups

Photoremovable protecting groups have found various applications in a number of diverse fields, such as neuroscience, photorelease of second messengers, peptides and proteins, two-photon excitation, x-ray crystallography and many others. In this chapter, several most significant and most illustrating examples are discussed.

1.2.1. Photorelease of neurotransmitters

One of the fields where photoactivatable molecules have been most extensively (and successfully) applied is that of the neurosciences. This broad area of research has been covered in several reviews[6,31,32] so only a brief introduction and a few examples of recent development are mentioned here.

Many clinically important compounds such as tranquilizers and antidepressants as well as abused drugs such as cocaine affect the reception functions of membrane bound proteins. Other receptor proteins regulate the transmission of signals between the cells of the mammalian central nervous system and between nerve and muscle cells. A neurotransmitter binds to a specific surface cell receptor, which thus causes a transient (usually in μs or ms time domain) rearrangement of the latter and formation of channels (ligand-gated ion

channels), through which small inorganic molecules can cross membranes of neural or muscle cells, thus giving rise to a transient voltage across it. Measuring this voltage is very informative about the function of the particular receptor. There are several electrophysiological methods used in observing such processes. Among them is pulsed laser photolysis which employs photolabile precursors of the neurotransmitters. Ppg's are used to block a particular functional group within the neurotransmitter and by doing so convert it into a biologically inert molecule. Mixing of the protected substance and the cells does not produce any physiological response in the receptor. Later, the cell is irradiated with a short pulse of light, the active substance is released and the physiological response of interest can be measured with a time resolution restricted only by the rate of deprotection of the ppg. This technique has proved that the time needed for the current to reach its maximum is much shorter than the time found in other experiments, such as cell flow technique. Many photoactivatable precursors of neurotransmitters (glutamates, γ-aminobutyric acid, caged glycine, carbachol *etc*.) have been synthesized.

Neurotransmitters can be roughly categorised as amino acids (glutamic acid, aspartic acid, GABA), peptides (vasopressin, neurotensin) and monoamines (dopamine, norepinephrine).

Glutamate is the major excitatory neurotransmitter in the vertebrate central nervous system. It has been used for mapping neuronal activity, probing neural connectivity, probing neuronal integration and synaptic plasticity. Few examples of glutamate caged with different ppg's are shown in the Scheme 9.

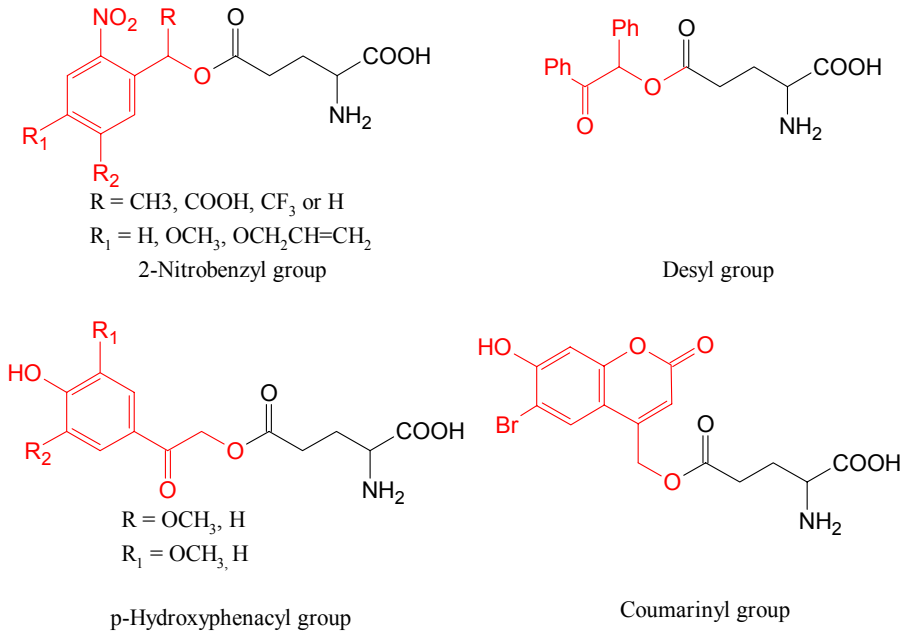

Scheme 9. Examples of protected glutamate.

About 24 different derivatives of caged glutamate have been synthesized and employed in biological studies[11], emphasizing the need of finding an ideal probe for glutamate. The glutamate molecule has three different functional groups that can be protected. These are the α and γ-carboxylic functions as well as the amino group. All of the applied ppg's have advantages and disadvantages. The nitrobenzyl class shows relatively slow rates of release. The hydroxyphenacyl ppg releases the substrate much faster than the nitrobenzyl one and with the satisfactory quantum yield, but the extinction coefficient at wavelengths above 300 nm is low. The desyl series performs very poorly, and only the γ-derivative undergoes the desired fragmentation but with a very low photolytic efficiency at higher wavelength of irradiation.

An interesting example of glutamate caged with hydroxyphenacyl group is the work of Kandler *et al.*[19] They studied the mechanisms of mapping synaptic plasticity (SP) of brain cells. Synaptic plasticity is a nervous system phenomenon that represents variability of the strength of a signal transmitted through a synapse. It is part of the Hebbian theory about the neurochemical foundations of memory and learning. The memory storage in the brain as well as the ability of the neural system to adapt to novel situations are thought to be closely related to SP. Using caged glutamate Kandler managed to introduce long-term depression

(LTD) in the postsynaptic part of the synapses and this way clarified that LTD but not LTP (long-term potentiation), is induced by stimulated neurotransmitter release and is purely postsynaptic.

1.2.2. Photorelease of second messengers

If we refer to a hormone or neurotransmitter as the 'first messenger', when it binds to the external domain of a receptor causing a change in the level of an intercellular regulatory molecule that triggers cell responses, that would be then 'second messenger'. Second messengers also greatly amplify the strength of the signal. Three major classes of second messengers can be distinguished: calcium ions, cyclic nucleotide monophosphates and inositol triphosphate and diacylglycerol.

Calcium ions Ca^{2+} are probably the most widely used intracellular messengers and the rise in the concentration of Ca^{2+} in the cytosol triggers many different responses such as muscle contraction, release of neurotransmitters at synapses, secretion of insulin, activation of T and B cells when they bind antigen, adhesion of cells to the extracellular matrix, variety of biological changes mediated by protein kinase C *etc.* There are two main depots of Ca^{2+} for the cell: the extracellular fluid and the endoplasmatic reticulum. Nevertheless, its level in the cell can substantially rise when channels in the plasma membrane open to let it in from the extracellular fluid or from the depots within the cell.
Photolabile Ca^{2+}-chelators are used to define its role by rapid concentration jumps following a short laser pulse. Caged calcium reagents are unique among the cage compounds as release of Ca^{2+} depends on the change in the affinity of a photolabile chelator agent upon irradiaton. A few commercially available Ca^{2+}-chelators are shown in the Scheme 10.

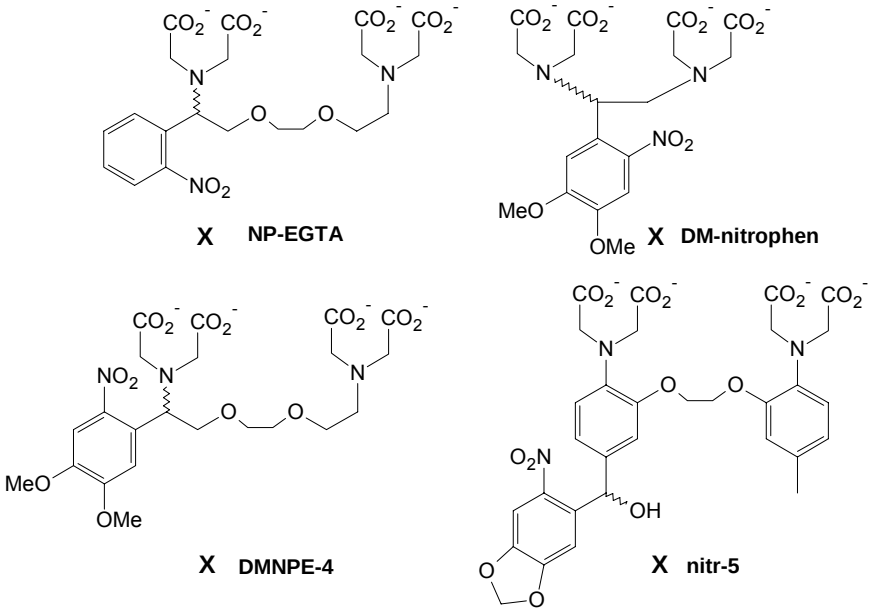

Scheme 10. Calcium chelators commercially available.

The cyclic nucleoside monophosphates, adenine- and guanidine-3,5-cyclic monophosphates (cAMP, cGMP), control a variety of cellular processes. Cyclic AMP is a second messenger used for intracellular signal transduction such as transferring the effects of hormones like glucagon and adrenaline, which cannot pass through the cell membrane. Its main purpose is that of activating the protein kinases and regulate the passage of Ca^{2+} through ion channels. Cyclic GMP acts much like cAMP, mostly by activating intracellular protein kinases in response to the binding of membrane-impermeable peptide hormones to the external cell surface. Caged cAMP and cGMP are very useful in studding signaling pathways in cells. The cyclic nucleotides are rendered inactive by esterification of the free phosphate moiety by several photoremovable protecting groups, with 2-nitrobenzyl and the coumarinyl derivatives being the most used ones (Scheme 11 and 12, respectively).

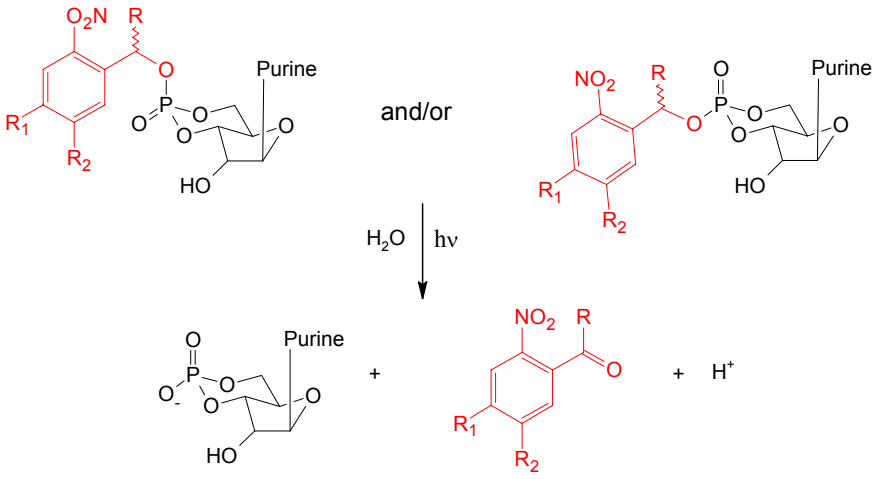

DMNB-caged cAMPs R = H, $R_1 = R_2 = OCH_3$, Purine = adenin-9-yl
DMNB-caged cGMPs R = H, $R_1 = R_2 = OCH_3$, Purine = guanin-9-yl
BCMCNB-caged cAMPs R = R_2 = H, $R_1 = CON(CH_2COOH)_2$, Purine = adenin-9-yl

Scheme 11. Photolysis of 2-nitrobenzyl-caged cNMPs.

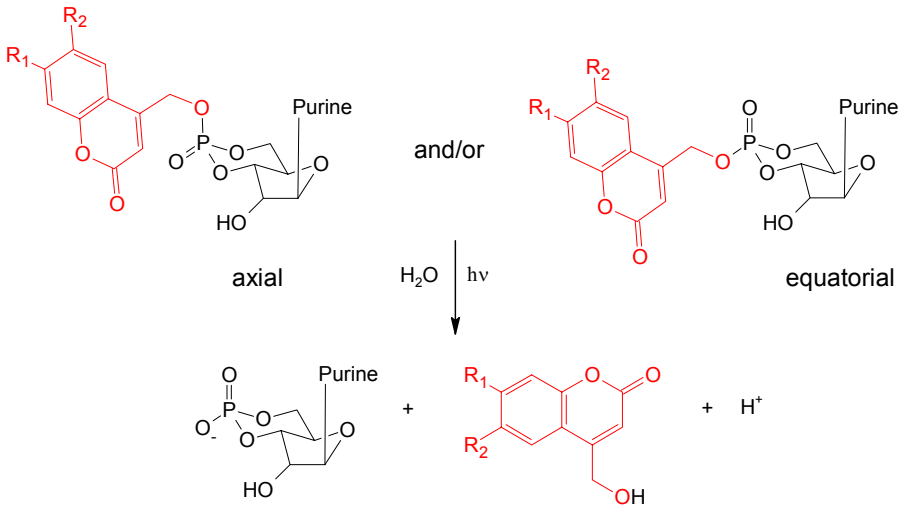

DMCM-caged cAMPs $R_1 = R_2 = OCH_3$, Purine = adenin-9-yl
BCMCM-caged cGMPs $R_1 = R_2 = OCH_2COOH$, Purine = guanin-9-yl
BECMCM-caged cAMPs $R_1 = R_2 = OCH_2COOEt$, Purine = adenin-9-yl

Scheme 12. Photolysis of coumarinylmethyl-caged cNMPs

Cyclic AMP and GMP have as main targets cyclic nucleotide-gated channels, cGMP- and cAMP dependent kinases, and regulated phosphodiesterases, guanisinenucleotide exchange

factors and bacterial transcription factors. An interesting example of the use of BECMCM caged cAMP and cGMP is the work of Kaupp and co-workers[33]. They investigated the Ca^{2+} influx in sperm. The egg and the sperm meet through a process called chemotaxis. The sperm uses chemical gradients of a specific chemo-attractant in order to locate the egg. The egg releases a chemical compound that binds to the outer shell of the sperm, causing a Ca^{2+} influx to the cell. This then changes the beating patterns of the tail of the sperm in thereby introduces correction in its trajectory of movement. Kaupp demonstrated that Ca^{2+}-channels are open through cGMP, making it in this way a primary messenger. This is a significant discovery correcting the model underlying the process of chemotaxis that was made possible by the use of ppg's.

1.2.3. Photorelease of peptides and proteins

Peptides have a wide range of biological activities and function, such as hormones and neurotransmitters. Synthetic peptides can be used as selective inhibitors of protein activity. Thus, photoactivatable peptides have huge potential for application. The design involves identification of amino acid substitution patterns that inhibit peptide activity, for example preventing the peptide from binding to a target protein.

One of the approaches to introduce an amino acid previously protected with a photolabile protecting group at the desired position is using solid-phase peptide synthesis. Walker *et al.* [34] used this method to introduce nitrobenzyltyrosine into RS-20, a target peptide for calmodulin, which binds calcium and is involved in many Ca^{2+} mediated events. The affinity of the caged RS-20 for calcium-calmodulin was 50 times lower than that of RS-20. The system was used to study the role of the calcium-calmodulin complex and myosine II in the rapid locomotion of newt eosinophils (leukocites). Similiarly, Tatsu and co-workers[35] synthesized caged neuropeptide Y (NPY), a 36-amino acid peptide that contains 5 tyrosine residues, two of which are at the N- and C-termini. NPY is thought to play an important role in the processes of blood pressure regulation, anxiety and feeding disorder. 2-Nitrobenzyl-tyrosine was introduced at either one or both termini, and asses that biological activity was reduced by one order of magnitude in the mono-protected peptides, and two orders of magnitude upon introduction of nitrobenzyl groups at both ends. The activity was promptly

restored upon UV irradiation. The structure of the 2-nitrobenzyl caged tyrosine is shown in the Scheme 13.

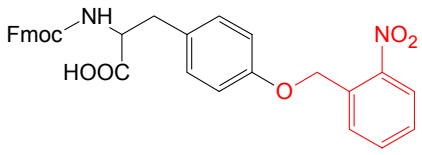

Scheme 13. Caged tyrosine residue.

A combination of solid-phase synthesis (SPS) and photolithography is called microarray fabrication. This technique consists of attaching protected building blocks to a solid support and irradiating them through a mask, thereby leaving some of the molecules unchanged and deprotecting others. The free functional groups are then made to react with other building blocks. Repetition of the irradiation through masks with different patterns and coupling steps leads to the desired set of products. Microarrays prepared by *in situ* synthesis are thus examples of spatially addressable combinatorial libraries. Quite a few ppg's are suitable for this type of light directed combinatorial synthesis, including nitrobenzyl protecting group, dimethoxybenzoin group and nitrophenylpropyloxycarbonyl group. A good example is 5-phenoxyphenyl-NPPpoc group (Scheme 14). It exibits a half-time of deprotection of 16 s and a chemical yield of 98% that is superior to many other groups. A review on the microarray methodology is included in the book by Goeldner and Givens[11].

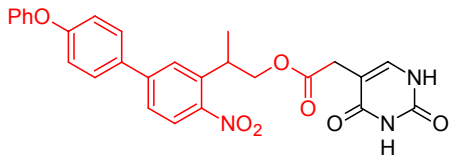

Scheme 14. 5-phenoxyphenyl-NPPpoc-group.

Dussy and collegues[36] developed a new photocleavable building block, consisting of a nucleic acid derived structure and 2-nitrobenzyl cage. The photochemistry of a single-stranded DNA, modified with the photocleavable building block, showed that site specific breaks can be easily introduced by irradiation with light above 360 nm. Their results are potentially applicable in several important research areas, such as studies of DNA strand

break/repair processes and DNA topology. The building block was incorporated into oligonucleotides, which were able to build stable DNA complexes.

1.2.4. Photoactivatable fluorophores

Photoactivatable fluorophores are molecules that yield a fluorescent species upon irradiation. They have been obtained by coupling a fluorescent dye to a photoremovable protecting group which prevents it from displaying its usual emission. UV-irradiation frees the fluorescent species and restores its absorption and emission properties in the visible region. Typical examples are photoactivatable fluorescein, caged rhodamines and caged resorufin. Successful application of such compunds has been reported in many fields. The ability to easily monitor the formation of the deprotected substrate makes them useful calibration systems.

Caged resorufin coupled to G-actin was used as a photoactivatable fluorescent tracer by Theriot *et al.*[37] to investigate the intracellular motility of *Listeria monocytogenes*. This bacterium is a common food pathogen and, once inside the infected cell, rapidly induces polymerization of G-actin to filaments forming 'comet tails', which quickly propel it through cytoplasm. Irradiation of the tails allowed monitoring of the movement and turnover of the labeled filaments by fluorescence videomicroscopy, giving useful insight into the general actin-based motility of pathogens within the cell.

Vincent and O'Farrell[38] applied a photoactivatable fluorescent tracer to the study of cell lineage during *Drosophila* embryos development. A nitrobenzyl-caged fluorescein was connected to a dextran backbone and the latter to a nuclear localization peptide. The dextran molecule served the purpose of preventing intercellular diffusion, whereas the peptide induced localization of the tracer at the nuclei to improve the physical separation among the targets and making it easier to distinguish the single cells. The compound was injected into the synctyal blastoderm, *i.e.* at the stage when the nuclei derived from the early mitotic divisions still reside in a common cytoplasm, allowing the tracer to diffuse and localize the nuclei. After the subsequent cellularization phase, when membranes from around each nucleus and the embryos acquire a cellular organization, single cells were fluorescence-labelled upon irradiation. This way the development during the subsequent steps could be

followed. The method is suitable for application in live specimens, so that 'movies' of gastrulating embryos can be recorded with a CCD camera.

There are many other successful applications but also some limitations of photoactivatable fluorophores. Caged fluorescein, for example, is highly hydrophobic, and most proteins tend to aggregate if they are labeled with it. Both caged resorufin and fluorescein are subject to photobleaching after activation, which causes problems in their imaging in cells.

1.2.5. Two-photon excitation

One of the big advantages of using photoactivatable compounds in the investigation of biological systems is the improved temporal and spatial resolution of the experiments by comparison to the other, more conventional methods. A further step in this direction is given by two-photon excitation of a photoactivatable compound, which is giving three-dimensional control over the localization of substrate release.[39]

In two-photon photolysis UV excitation is replaced by the simultaneous absorption of two IR photons of equivalent total energy. The probability of absorption is proportional to I^2 and to δ, where I is the light intensity and δ the two-photon absorption cross-section measured in GM (1 Göppert-Mayer = 10^{-50} cm^4 s $photon^{-1}$). Therefore, the event is confined to the small region near the laser focus and is negligible in the surrounding area, so that the release can be restricted to volumes smaller than a femtolitre.[40,41] Another advantage of this technique is that IR photons are less likely to cause photodamage to living tissue. Still, some precautions have to be taken. The toxicity from the irradiation is related to the laser power, and an upper limit of 5-10 mW was established in the systems investigated.[42,43]

Nevertheless, successful two-photon uncaging of calcium from azid-1 and glutamate from a coumarinyl derivative has been achieved by Brown *et al*.[41]. They compared the two-photon action cross sections of DM-nitrophen, NP-EGTA and azid-1. Azid-1 and DM-nitrophen had a maximum cross section of ~1.4 GM at 700 nm and ~0.013 GM at 730 nm, respectively. NP-EGTA did not show any detectable uncaging signal. It was calculated that a 10 μs pulse train of ~ 7 mW at 700 nm would photolyze all azid-1 within the focal volume, whereas DM-nitrophen would need about 74 mW at 730 nm in the same conditions, a value prone to cause

damage to the biological environment. Yet, DM-nitrophen has been used to generate spatially-confined artificial Ca^{2+} sparks inside cardiac myocytes.[44]

1.3. Photochemistry of 9-fluorenol

The photochemistry of 9-fluorenol (FOH) is well known. The photodecomposition of FOH has been studied in polar and non-polar solvents by use of laser flash photolysis with a time resolution of 10 ps. The initial studies were carried out by Wan and Krogh who found that 9-fluorenol undergoes a relatively efficient reaction on irradiation in aqueous methanol resulting in production of 9-methoxy-fluorene as shown below. [45,46]

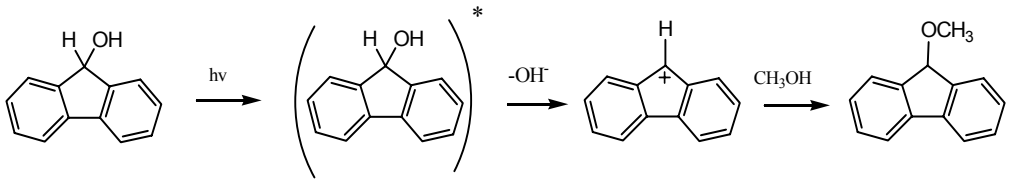

This substitution was proposed to occur *via* C-OH heterolysis of the singlet excited state of the alcohol leading to the 9-fluorenyl cation, followed by trapping with methanol. The heterolysis appears to occur despite the hydroxide ion being a poor leaving group. Alcohols such as diphenylmethanol that lack the central ring of the fluorenyl system do not undergo this photoreaction, or do so with considerably less efficiency. This led to the proposal that the 9-fluorenyl cation forms in the fluorenyl systems because of an enhanced reactivity of excited states leading to internal cyclic arrays containing 4n-π systems.[45-47]

The easy formation of the 9-fluorenyl cation is surprising in respect not only to the poor leaving group, but also in that these types of cations are somewhat destabilized in the ground state. This can be seen in solvolysis reactions proceeding *via* 9-fluorenyl cations that occur several orders of magnitude slower than those of analogues lacking the central ring[48].

Initial flash photolysis studies with 9-fluorenol were performed by Mecklenburg and Hilinski.[49] They found that the 9-fluorenyl cation, F^+ (appearing at 515 nm), is extremely short-lived in aqueous solution, forming and decaying within the laser pulse on a picosecond apparatus in < 25 ps. With the less nucleophilic 1,1,1,3,3,3-hexafluoroisopropanol (HFIP) as

a solvent, the lifetime increases by over six orders of magnitude to 10 μs[50]. The solvent HFIP has a dramatic kinetic stabilizing effect. This has been exploited to observe a number of cations that are relatively reactive and, consequently are very short lived in solvents such as water, methanol and ethanol. The 9-fluorenyl cation has reactivity towards the solvent HFIP that lies between that of cumenyl cation and the phenethyl cation. We will be back to the polyfluorinated alcohols as solvents with specific properties later in this chapter.

Mecklenburg and Hilinski have also detected an additional absorption band at 500 nm, which they identified as the fluorenyl radical, F$^{\cdot}$ thus supporting the conclusions of Wan *et al.* on the occurrence of photoheterolysis as well as photohomolysis. The lifetime of F$^{\cdot}$ in aqueous methanol appears to be unusually long (> 1μs).

In contrast to this interpretation, Gaillard *et al.*[51] assigned a broad and long-lived (> 6 μs) band with maximum at 640 nm to the cation, F^+. This assignment, however, was corrected[50] on the basis of nanosecond laser flash photolysis experiments in which F^+ was generated specifically in the weakly nucleophilic solvent HFIP (in which the longevity of F^+, absorbing at 515 nm, is a record 30 μs).

Taking all these data together, it is evident that electronically excited FOH undergoes two different reactions, both involving the C9–OH bond, namely homo- and heterolytic cleavage. It also appears that these reactions are strongly solvent dependent. Protic solvents react with a given cation in the order methanol > ethanol > water >> TFE >> HFIP. These effects are large (see Table 1 for 9-fluorenyl), and in many cases can be exploited to increase the lifetime into a range where a particular cation becomes detectable by slower techniques[52].

	H_2O	CF_3CH_2OH	$(CF_3)_2CHOH$
9-fluorenyl	$>4 \times 10^{10}$	8×10^{8}	2×10^{4}

Table 1. Effect of solvent on rate constants k_s (s^{-1}, 20 °C) for decay of 9-fluorenyl cation.

In solvents with high polarity, such as 1,1,1,3,3,3-hexafluoroisopropanol (HFIP), 2,2,2-trifluoroethanol (TFE), formamide or water, the fluorenyl cation, F^+, forms by heterolytic C–O bond cleavage (Figure 1).

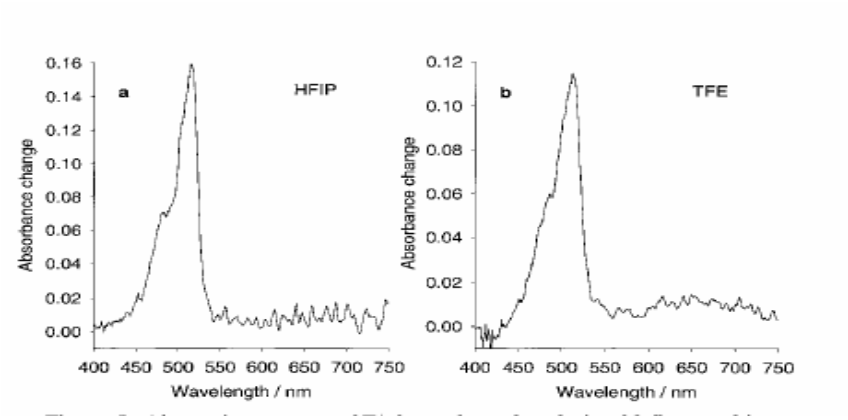

Figure 1. Absorption spectra of F^+ formed on photolysis of 9-fluorenol in a) HFIP and b) TFE. [53]

In water, the initial (10 ps) spectrum of F^+ has λ_{max} at < 460 nm. This absorption red-shifts with τ = 25 ps to the "classical" spectrum with a sharp maximum at λ_{max} = 510–515 nm. The shift is assigned to the solvation of the initially "naked" cation, or rather, the contact ion pair. The lifetime of the solvated fluorenyl cation in water (or D_2O) and TFE was measured to be τ = 20 ps and 1ns, respectively. As far as heterolysis is concerned, it is evident that in order for solvation to influence the reaction, the solvation of the incipient ions must be very rapid. This implies that the solvent must play an active part in the early stages of the bond-breaking process. In solvents of lower polarity such as alkanes, ethers and alcohols, the long-lived ($\tau_{1/2}$ $\approx$1 μs) fluorenyl radical, F˙, (λ_{max} = 500 nm) forms through homolytic C–O cleavage. In addition to the radical and cation, the vibrationally relaxed excited singlet state of FOH is seen with its absorption at $\approx$ 640 nm (Figure 2); its lifetime is strongly dependent on the solvent, ranging from 10 ps for formamide to 1.7 ns for cyclohexane, as is evident from the Table 2. The rate constant for singlet decay increases exponentially with the polarity of the solvent or with the Gutmann solvent acceptor number. The relaxation of S_1 to S_0 is accompanied by homolytic C9–O bond cleavage. The exception are solvents HFIP, TFE and water, where S_1 is not seen. It is assumed that in these cases τ_s is much less than 10 ps.[53]

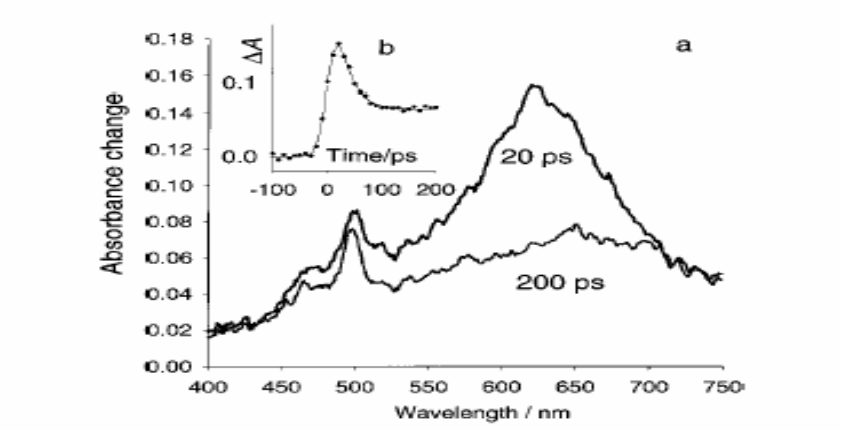

Figure 2. a) Absorption spectra of the transients recorded at 20 and 200 ps after the 266 nm excitation pulse and b) the decay kinetics monitored at 630 nm in a solution of 9-fluorenol in methanol. [53]

Solvent	Polarity[a]/E_T^N	dielectric constant ε_r	λ_{max} of the $S_1 \rightarrow S_n$ transition	τ_s [ps][b]
2,2,2,2',2',2'-hexafluoroisopropanol	1.068	16.6	not detected	< 10
water	≡ 1.000	78.3	not detected	< 10
2,2,2-trifluoroethanol	0.898	26.7	not detected	< 10
glycerol	0.812	42.5	650	20
formamide	0.799	111.0	660	10
ethylene glycol	0.790	37.7	650	36
MeOH	0.762	32.66	630	30 (20[c])
N-methylformamide	0.722	182.4	650	40
EtOH	0.654	24.55	630	50 (20[c])
*n*PrOH	0.617	20.45	630	110
*i*PrOH	0.546	19.92	630	70 (200[c])
MeCN	0.460	35.94	620	130 – 160 (350[2], 400[c])
dimethylformamide	0.404	36.71	640	540
tert-butanol	0.389	12.47	630	150 – 290
dichloroethane	0.327	10.37	630	100
dichloromethane	0.309	8.93	630	30
1,2-dimethoxyethane	0.231	7.2	630	1000
THF	0.207	7.58	645	1300 (1500[bd])
dioxane	0.164	2.21	640	1200 (1200[bd])
dimethoxymethane	0.157	2.65	630	800 (1100[bd])
cyclohexane	0.006	2.02	625	1700 (1900[bd])

Table 2. The lifetime of FOH (S_1), τ_s, in different solvents, air-saturated, as determined by the decay of the S_1 to S_0 absorption signal. [53]

As mentioned earlier, it has been realized that carbocations can be remarkably long-lived in solvents such as HFIP and, to a certain extent, TFE. This interesting behavior of both 9-

fluorenol and its derivatives upon photolysis in polyfluorinated alcohols can be explained by having a closer look into the properties of these solvents.

1.3.1. The polyfluorinated alcohols case

The polyfluorinated alcohols appear to be an interesting group of electrolyte solvents exhibiting properties distinct from other hydrogen-bonding solvents. Electrolyte conductance in 2,2,2-trifluoroethanol (TFE) shows a pattern consistent with poor cation solvation and good solvation of anions. This is a consequence of the electron-withdrawing ability of the CF_3 group, which causes diminished basicity and nucleophilicity of the alcohol oxygen but increased acidity of the proton. This characteristic of the fluorinated alcohols makes them one extreme in a spectrum of ion-solvent interactions. In contrast to the fluoro alcohols, the dipolar aprotic solvents interact strongly only with cations. Between these two extremes lie the alcohols, amides, and water which possess both acidic and basic sites, leading to effective solvation of both cations and anions[54]. It is helpful to compare the properties of these solvents to those of 2-PrOH, their hydrocarbon analog. Pertinent data are summarized in Table 3.

As compared to TFE and 2-PrOH, HFIP exhibits lower viscosity, boiling point and entropy of vaporization, all of which point to considerably less intermolecular hydrogen bonding in HFIP. However, not only is HFIP more acidic, but formation of a hydrogen-bonded complex between acetone and HFIP is far more exothermic than acetone-TFE, a difference of 2.2 kcal/mol. In view of its greater effectiveness as a hydrogen bond donor, the minimal degree of intermolecular hydrogen bonding in HFIP attests to its unsuitability as a hydrogen acceptor. This is also reflected by the fact that although the compound is highly acidic in water, its autoprotolysis constant is low enough not to interfere with conductivity measurements, the specific conductance of HFIP being at most 7×10^{-9} $cm^{-1}ohm^{-1}$.

	HFIP	TFE	2-PrOH
ρ^{25}	1.605[a]	1.383[f]	0.781[f]
ε / mol· dm^{-3}	16.7[a]	26.7[g]	19.4[k]
D / Debyes	2.05[b]	2.03[b]	1.68[i]
H / cP	1.62[a]	1.78[g]	2.08[f]
pK_A water	9.30[c]	12.37[h]	~ 17[m]
ΔH form, acetone complex in CCl_4 / kcal · mol^{-1}	-5.94[d]	73.75[f]	82.5[f]
Boiling point / ^{o}C	58.6[a]	73.75[f]	82.5[f]
Entropy of vaporization, Gibbs / J · K^{-1}· mol^{-1}	26.2[e]	-3.72[d]	28.3

Table 3. Properties of HFIP; TFE and 2-Propanol. [54]

[a] J. Murto, A. Kivinen, S. Kivimaa, *Suom. Kemistilehti B,* **40,** 250 (1967). [b]A. Kivinen, J. Murto, and L. Kiilpi, *Suom.* Kemistilehti 6, **40,** 336 (1967). [c]W. J. Middleton and R. V. Lindsey, Jr., *J.* Amer. Chem. Soc., **86,** 4948 (1964). [d]**A.** Kivinen, J. Murto, and L. Kilpi, *Suom.* Kemistilehti *6,* **40,** 301 (1967). [e]Calculated from data in J. Murto and **A.** Kivinen, *ibid.,* **40,** 258 (1967). [f]Reference 4. [g]J. Murto and E. Heino, *Suom.* Kemistilehti *6,* **39,** 263 (1966). [h]P. Ballinger and **F. A.** Long, *J.* Amer. Chem. Soc., **81,** 1050 (1959); **92,** 795 (1960). [i]Pennsalt Chemicals Corp., "Trifluoroethanol," Booklet No. DC-1254, Philadelphia, Pa., 1956. [i]Reference 18. [k]W. Dannhauser and L. W. Bahe, .I. Chem. Phys., **40,** 3058 (1964). Taken from NBS Circular No. 537. [m]Estimated.

In conclusion, HFIP and TFE are members of a solvent class distinctly different from other hydrogen-bonding solvents which interact with both cations and anions, and opposed to dipolar aprotic solvents which solvate cations preferentially.

2. Problem statement

The aim of this project was to prepare and study a system for the photochemical release of methanol. Our idea is based on the photochemistry of 9-fluorenol, which is well established and described in the introductory chapter of the present work. This would be useful in biology knowing that instead of methanol one could have choline or any other alcohol-containing molecules with a potential biological function, such as glucose or folic acid.

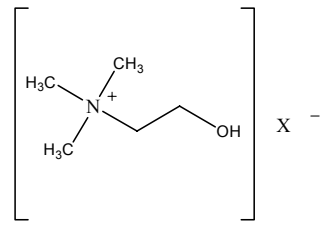

X = chloride, hydroxide, tartrate

Choline

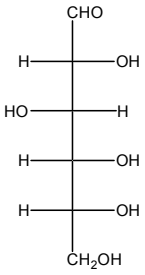

Glucose

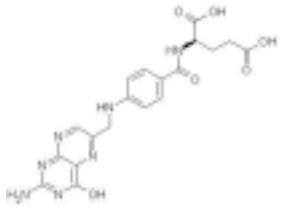

Folic acid

Choline is a quaternary saturated amine that acts as a nutrient, essential for cardiovascular and brain function and for cellular membrane composition and repair.

Choline and its metabolites are needed for three main physiological purposes: structural integrity and signaling roles for cell membranes, acetylcholine synthesis and as a major source for methyl groups via its metabolite, trimethylglycine (betaine) that participates in the S-adenosylmethionine synthesis pathways. Protecting groups are designed first to mask the biological function and second to permit the liberation in a controlled way. In this manner, caged choline (photolabile precursor) can be used to study the mechanism of choline release from the enzyme active site[55].

Many photoremovable protecting groups have been developed for alcohols, such as ester and ether derivatives, to modulate their acid and base sensitivity[1]. A series of carbamates[56], carbonates[57] and acetals[58-60] have also been described. They each have their own photochemical properties (slow release of CO_2) but also represent chemical functionalities of

restricted hydrolytic stability. Orthogonality of protecting groups was also developed for alcohols[61-63] to extend their synthetic use.

Because of its importance in biology and in organic synthesis, we got prompted to investigate the possibility of extending alcohol protecting groups to a new class of derivatives. Our idea is to study the photochemistry of 2,7-diamino-9-fluorenol derivatives in various solvents by steady-state irradiation and laser flash photolysis in order to establish product distributions and to observe transient intermediates. We have opted for these particular compounds based on the fact that the photochemistry of parent 9-fluorenol is fairly well established (described in the next chapter of the present work), whereas the introduction of the amino substituents is expected to enhance the photochemically desired properties (mentioned in detail in the introduction). In particular, adding amino groups in positions 2 and 7 should favor cation (F^+) over radical formation. The cation formation is more biocompatible whereas the radical one should always be avoided in living tissues as it is very damaging.

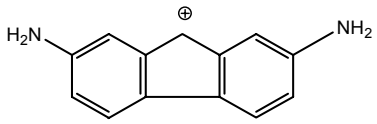

The second advantage of this substitution with two amino groups is that it makes the cation longer lived and therefore easier to observe. Furthermore, this shifts the absorption of the chromophore towards the visible area of the spectrum and allows for biologically less damaging illumination by light of suitable wavelengths. Water-solubility is also improved in comparison to that of the parent compound, important characteristic for a photoprotected substrate that should be soluble in aquous buffered media in living tissues.

Before studying the photochemical properties of 2,7-diamino-9-fluorenol, we will describe the synthesis of 2,7-diamino-9-fluorenol and two of its derivatives.

3. Synthesis

3.1. Synthesis of 2,7-diamino-9-fluorenol

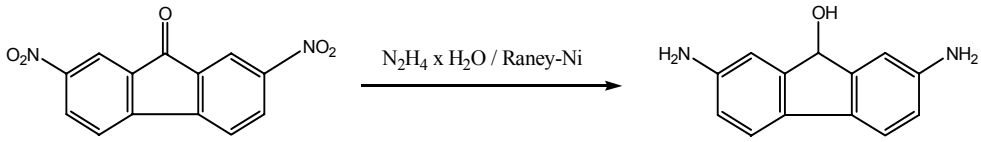

Scheme 15. Synthesis of 2,7-diamino-9-fluorenol

Reduction with hydrazine hydrate in hot ethanol using Raney nickel as a catalyst is a very convenient method for the preparation of aromatic amines from the corresponding nitro compounds.[64] Carbonyl groups are generally unaffected in this reaction. However, by employing a large excess of hydrazine hydrate (~ 100 molar equivalents) and a considerable amount of catalyst, the keto group gets reduced to the alcohol one allowing for preparation of aminofluoren-9-ols from the corresponding nitrofluorenones in good yields.[65]

2,7-Dinitrofluorenone (4 mmol) was dissolved in boiling 95% ethanol (400 ml). The hot solution was mixed with 85% hydrazine hydrate (10 ml) and Raney nickel[66] (0.2 g, wet weight), and heated on the oil bath for 30 min. After the addition of a second portion (10 ml) of hydrazine hydrate, the mixture was stirred and heated for another 30 min and filtered hot through celite. The progress of the reaction was monitored by TLC. The filtrate was concentrated, diluted with water, and the 2,7-diamino-9-fluorenol was collected by filtration. Crude product was purified by recrystallization from warm ethanol with active charcoal to yield light orange flakes.

Mol. formula/ Mol. Weight: $C_{13}H_{12}N_2O$ / 212.09 g/mol

Yield: 0.38 g (42 %)

TLC: R_f = 0.37 (Aluminum oxide neutral, EtOAc), R_f = 0.54 (Aluminum oxide neutral, EtOAc:MeOH = 95:5)

^{1}H NMR (400 MHz, *DMF*-d_7, *δ*/ ppm): δ 7.20 (d, 2H, J=8.0Hz, *H5* and *H4*), δ 6.89 (d, 2H, J=1.9Hz, *H8* and *H1*), δ 6.60 (dd, 2H, J=2.1Hz, J=8.0Hz, *H6* and *H3*), δ 5.31 (d, 1H, J=8.2Hz, *H9*), δ 5.26 (d, 1H, J=8.2Hz, *OH*), δ 5.04 (s, 4H, NH_2).

A representative spectrum is shown in Figure 3.

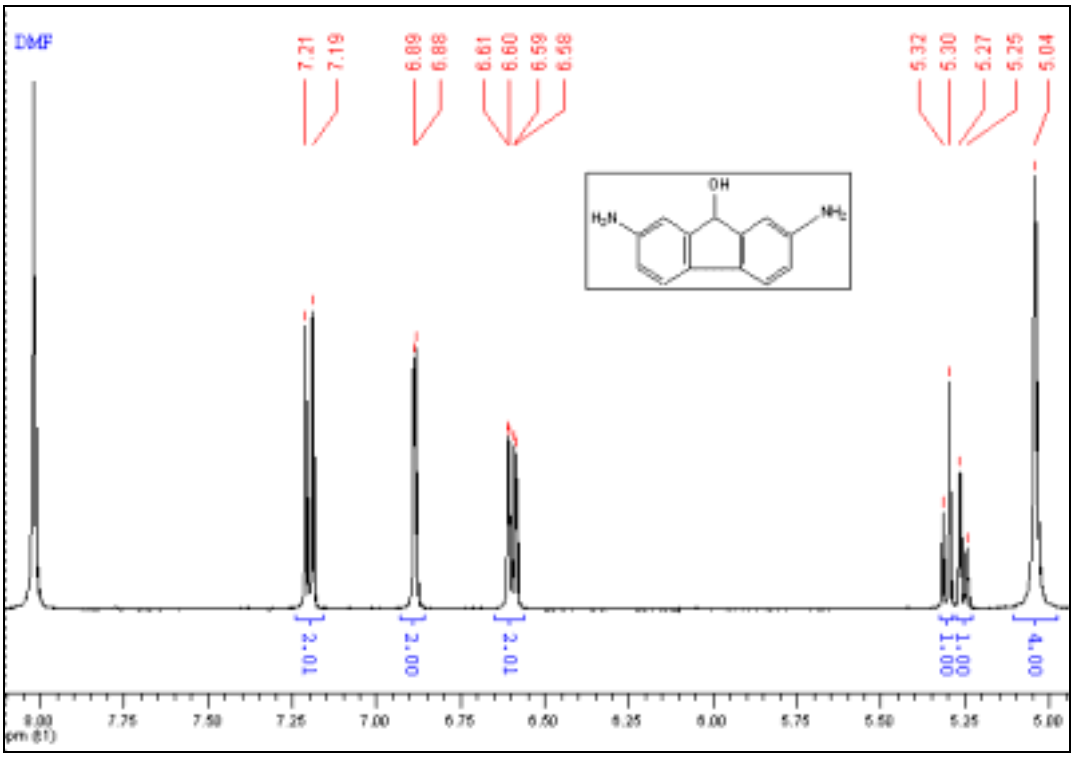

Figure 3. ^{1}H NMR spectrum (400 MHz, *δ*, *DMF*-d_7, 25°C) of 2,7-diamino-9-fluorenol.

^{13}C NMR (400 MHz, *DMF*-d_7, *δ*/ppm): 75.2 (C9), 112.0 (C3 and C6), 114.3 (C1 and C8), 119.2 (C4a and C4b), 131.0 (C4 and C5), 148.2 (C8a and C8b), 148.6 (C2 and C7).

GC/MS ($(CH_3)_2CO$, *m/z*): M^+ 212, 195.

mp.: 216-218 ºC

UV-Vis (H_2O, $c = 2 \cdot 10^{-5}$ mol · dm^{-3}): λ_{max} ~ 302 (20561) nm (ε / dm^3 ·mol^{-1} cm^{-1}).

UV-Vis (ACN, $c = 3.7 \cdot 10^{-5}$ mol · dm^{-3}): λ_{max} ~ 307 (24193) nm (ε / dm^3 ·mol^{-1} cm^{-1}).

As shown in Figure 4, the absorbance maximum of 2,7-diamino-9-fluorenol is shifted towards the visible area in respect to 9-fluorenol (302 nm and 270 nm, respectively), which was one of the aims of synthesizing the diamino derivative of the parent compound.

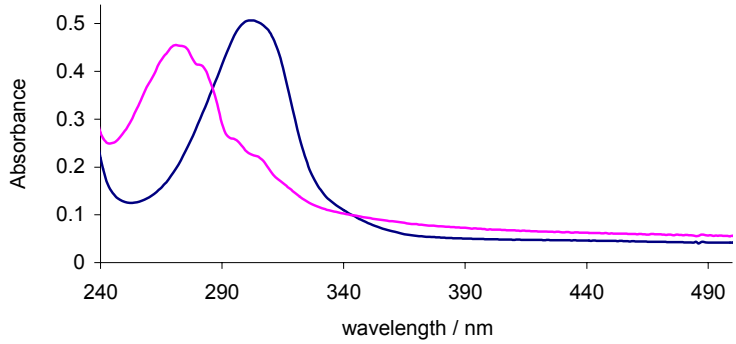

Figure 4. Absorption spectra of 2,7-diamino-9-fluorenol (blue) and 9-fluorenol (pink), λ_{max} = 305 nm and λ_{max} = 270 nm, respectively, in water.

3.2. Synthesis of 2,7-diamino-9-fluorenol derivatives

2,7-diamino-9-fluorenyl acetate and 2,7-diamino-9-fluorenyl ether are of interest to us in order to study the quantum yield of formation of 2,7-diamino-9-fluorenol. Several pathways such as copper-catalyzed etherification of aryl iodides[67] and cobalt-catalyzed acetylation of alcohols[68] have been tried in order to prepare these derivatives but have not been entirely successful. Here we describe briefly two attempts.

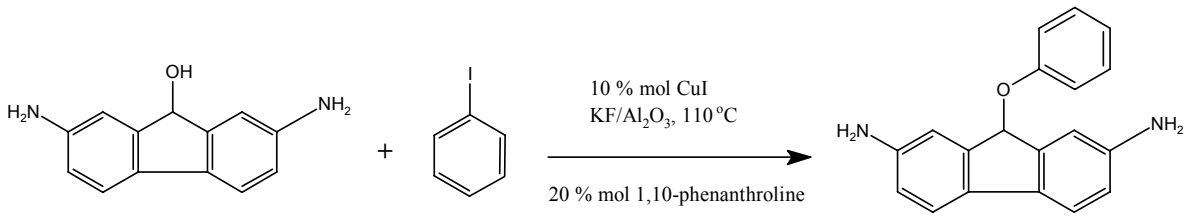

Scheme 16. Attempted synthesis of 2,7-diamino-9-fluorenyl phenyl ether.

To a solution of 21.2 mg of 2,7-diamino-9-fluorenol (0.1 mmol, 30 equiv) and 0.68 mg of phenyl iodide (0.0034 mmol, 1 equiv) under argon atmosphere were added 0.06 mg of CuI (10 mol %) and 0.132 mg of phenanthroline (20 mol %) followed by 2.66 mg of KF/Al_2O_3 (5 equiv), and the mixture was stirred in a sealed vial for 14 hrs at 110 °C. The progress of the reaction was monitored by TLC. The reaction mixture was filtered and the filtrate concentrated under reduced pressure but the high temperature required for evaporating phenyl iodide also affected the product. Acid-base extraction was a more successful method employed for separating the desired compound from the reaction mixture. The crude product was purified by preparative chromatography on neutral aluminum oxide using EtOAc:MeOH = 95:5 as eluent. However, characterization of the compound did not give satisfactory results and other methods for synthesis were employed.

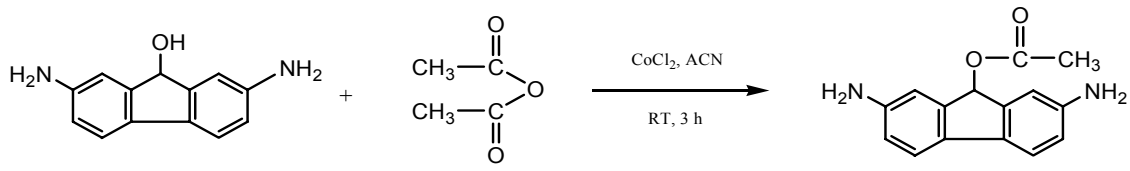

Scheme 17. Attempted synthesis of 2,7-diamino-9-fluorenyl acetate.

0.324 mg of anhydrous cobalt (II) chloride (5 mol %) was dissolved in dry acetonitrile and a mixture of 12.02 mg of acetic anhydride (2.5 equiv) and 10 mg of 2,7-diamino-9-fluorenol (0.05 mmol, 1 equiv) in dry acetonitrile added slowly over a period of 5 min at room temperature. The resulting mixture was stirred at ambient temperature under an atmosphere of nitrogen for 3.5 h. The progress of the reaction was monitored by TLC. The reaction mixture was evaporated in a rotavapour at 40-50 °C under reduced pressure. The silverish-green solid material was poured onto water ice and $NaHCO_3$ added to reach a pH of 7. The white amorphous solid easily precipitated and was collected by filtration. The crude product was separated by preparative chromatography on neutral aluminium oxide gel using EtOAc:MeOH = 95:5 as eluent. Again, following the characterization of the compound was not very clear whether we are having 2,7-diamino-9-fluorenol acetate.

Major drawback of both of the described synthesis was that etherification/acetylation was not occurring only in the 9-position of 2,7-diamino-9-fluorenol as expected, but the amino functions were undergoing the same reaction too. Mixtures of mono-, di- and tri-derivatives

were often obtained, as confirmed by GC/MS. Due to the difficulties encountered in separating the mixture and the very small amounts of starting material we had, this method was abandoned.

Few other attempts have been made, such as trying to synthesize the corresponding phosphate or diazo derivatives or introducing nitro groups in order to gain chemoselectivity for the etherification/acetylation reaction. However, the most successful route was a multi-step synthesis via the corresponding 9-diazo compound. The synthesis was carried out modifying the procedure of Guzik and Colter.[69]

The synthetic sequence starts with the known 2,7-dinitrofluorenone which is converted into the corresponding hydrazone in the presence of glacial acetic acid and hydrazine hydrate. The hydrazone is then oxidized by powdered silver oxide in THF yielding the diazo compound that is subsequently heated either in acetic acid or a phenol/benzene mixture in order to obtain the corresponding acetate and ether, respectively. Finally, the nitro group which acted as a protection is reduced by hydrazine hydrate in the presence of Raney nickel as a catalyst (Scheme 4). The sequence ketone $\rightarrow$ hydrazone $\rightarrow$ diazo compound $\rightarrow$ ether/acetate represents a useful method for obtaining 9-fluorenyl acetates and phenyl ethers. The details of the procedure follow.

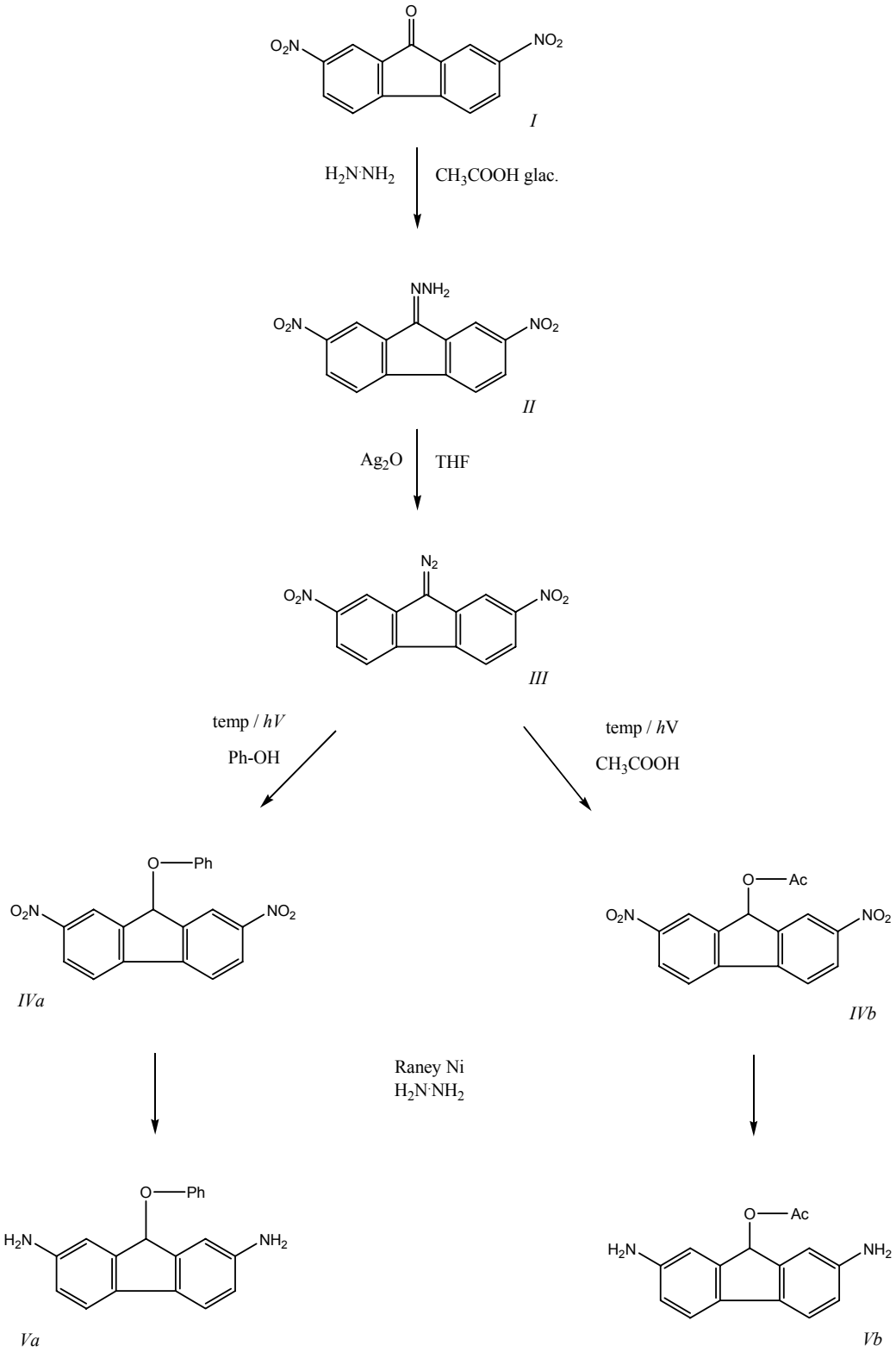

Scheme 18. Synthesis scheme for acetate and phenyl ether derivative of 2,7-diamino-9-fluorenol.

2,7-Dinitrofluorenone Hydrazone (II)

A 10 g of commercially available 2,7-dinitrofluorenone was dissolved in 700 ml of boiling glacial acetic acid and a solution of 10 ml of 100% hydrazine hydrate in 25 ml of glacial acetic acid was slowly added with stirring. The mixture was heated for an additional 15 min (orange amorphous precipitate after 5 min) and the cooled solution filtered, washed with water, and subsequently dried over phosphorous pentoxide in a vacuum-exicator.

Mol. formula/ Mol. Weight: $C_{13}H_8N_4O_4$ / 284.23 g/mol
Yield: 9.36 g (89 %)
TLC: R_f = 0.80 (Aluminium oxide neutral, EtOAc:MeOH = 90:10)
mp.: 280-283 ºC (decomp.)

9-Diazo-2,7-dinitrofluorenone (III)

In a three-necked flask equipped with an efficient stirrer and condenser, 9.3 g of II was dissolved in 500 ml of refluxing technical tetrahydrofuran. This suspension was oxidized with 14.5 g of powdered silver oxide. After it was refluxed for 5 h the warm solution was filtered and evaporated to one-third of its original volume. The brownish-orange material which separated was filtered and washed with 95% ethanol. Additional product was obtained by diluting the filtrate with water.

Mol. formula/ Mol. Weight: $C_{13}H_6N_4O_4$ / 282.21 g/mol
Yield: 3.75 g (42 %)
TLC: R_f = 0.74 (Aluminum oxide neutral, $CHCl_3$:MeOH = 20:1)
mp.: 196-199 ºC (decomp.)

2,7-Dinitro-9-fluorenyl Acetate (IVb)

To a hot solution (100-110 °C) of 50 ml of glacial acetic acid and 1 ml of 70% perchloric acid, 0.75 g of III was slowly added with stirring. After it was heated for an additional 5 min the solution was filtered and evaporated under reduced pressure to one-half of its original volume. The crystalline product which separated was filtered and washed with ether. Additional product was obtained by diluting the filtrate with an equal volume of water,

giving a total of 0.6 g (75%) of crude product. Crystallization from glacial acetic acid gave pale brown crystals.

Mol. formula/ Mol. Weight: $C_{15}H_{10}N_2O_6$ / 314.05 g/mol
Yield: 0.4g (49 %)
TLC: R_f = 0.75 (Aluminum oxide neutral, Hexane:EtOAc = 6:4)
mp.: 240 ºC (decomp.)
UV-Vis (ACN, c =1.0 · 10^{-5} mol · dm^{-3}): λ_{max} = 333 (45378) nm (ε / dm^3 ·mol^{-1} cm^{-1}).

2,7-Diamino-9-fluorenyl Acetate (Vb)
The procedure of reducing nitro groups was much the same as in the synthesis of 2,7-diamino-9-fluorenol mentioned previously in this chapter. 0.225 g of IVb was dissolved in boiling 95% ethanol (100ml). The hot solution was mixed with 85% hydrazine hydrate (1.75 ml) and Raney nickel (35mg, wet weight), and heated on the oil bath for 30 min. After the addition of a second portion (1.75 ml) of hydrazine hydrate, the mixture was stirred and heated for another 30 min and filtered hot through celite. The progress of the reaction was monitored by TLC. The filtrate was concentrated, diluted with water, and the 2,7-diamino-9-fluorenol acetate was collected by filtration. Crude product was purified by preparative chromatography using ethylacetate as eluent to yield a brownish powder.

Mol. formula/ Mol. Weight: $C_{15}H_{14}N_2O_2$ / 254.11 g/mol
Yield: 0.01 g (56 %)
TLC: R_f = 0.71 (Aluminum Oxide neutral, EtOAc), R_f = 0.46 (Aluminum Oxide neutral, Hexane:EtOAc = 6:4).
mp.: 165 ºC

^{1}H NMR (400 MHz, *DMSO*-d_6, δ/ppm): δ 7.18 (d, 2H, J=8.0Hz, *H5* and *H4*), δ 6.66 (d, 2H, J=1.7Hz, *H8* and *H1*), δ 6.52 (m, 2H, *H6* and *H3*), δ 6.42 (s, 1H, *H9*), δ 5.07 (s, 4H, NH_2), δ 2.12 (s, 3H, CH_3).
A representative spectrum is shown in Figure 5.

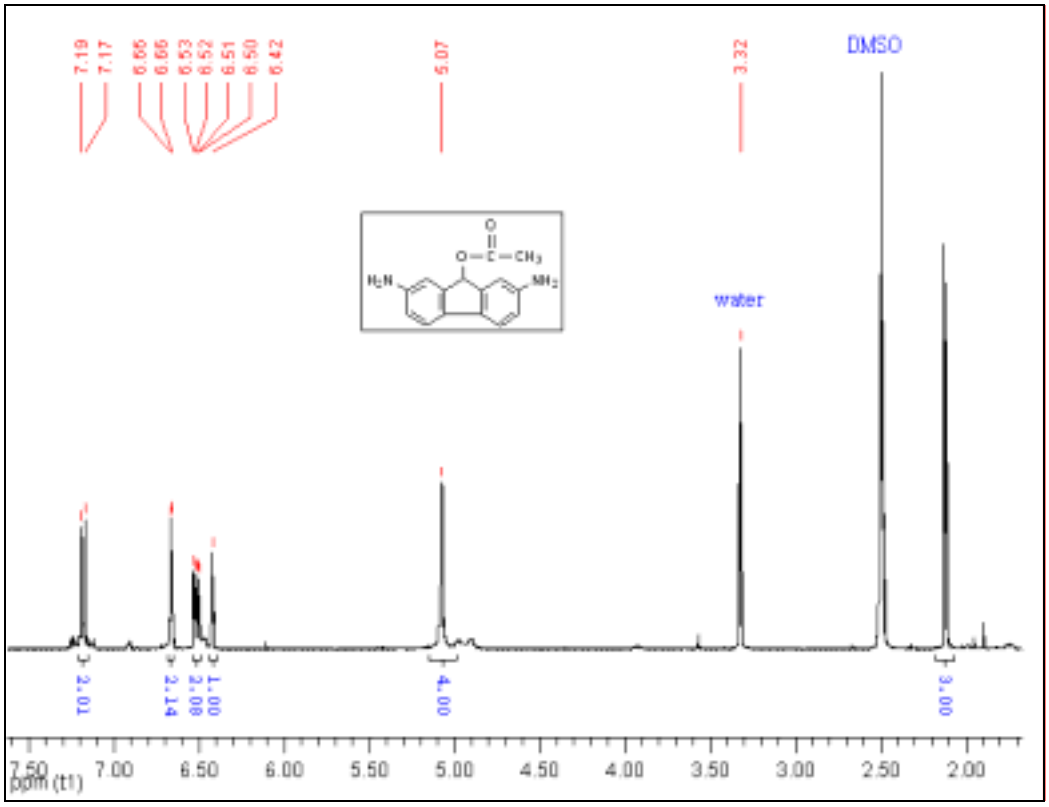

Figure 5. ^{1}H NMR spectrum (400 MHz, *δ*, *DMSO*-d_6, 25°C) of 2,7-diamino-9-fluorenyl acetate.

^{13}C NMR (400 MHz, *DMSO*-d_6, *δ*/ppm): 20.0 (**C**H_3CO), 76.8 (C9), 113.6 (C6 and C2), 115.5 (C8 and C1), 126.8 (C4a and C4b), 127.9 (C4 and C5), 142.3 (C8a and C8b), 146.8 (C2 and C7), 172.6 (CO).

GC/MS ($(CH_3)_2CO$, *m/z*): M^+ 254, 211,195, 167.

UV-Vis (H_2O, $c = 1.95 \cdot 10^{-5}$ mol · dm^{-3}): λ_{max} ~ 301 (34170) nm (ε / dm^3 ·mol^{-1} cm^{-1}).
UV-Vis (ACN, $c = 1.95 \cdot 10^{-5}$ mol · dm^{-3}): λ_{max} ~ 308 (47516) nm (ε / dm^3 ·mol^{-1} cm^{-1}).

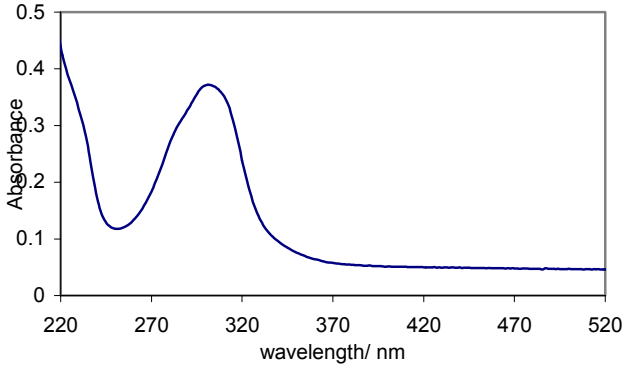

Figure 6. Absorption spectrum of 2,7-diamino-9-fluorenyl acetate (λ_{max} = 301 nm) in water.

2,7-Dinitro-9-fluorenyl Phenyl Ether (IVa)

The procedure was similar to that used for IVb. To a hot solution (100°C) of 10 g of phenol, 10 ml of benzene and 1 ml of 70% perchloric acid, 0.75 g of III was slowly added with stirring. After it was heated for an additional 5 min the solution was filtered hot. Shaking with aquous base (NaHCO3, pH ~ 10) and extracting the organic layer with ether yielded a black amorphous solid which was not further purified but reduced crude in the next step.

Mol. formula/ Mol. Weight: $C_{19}H_{12}N_2O_5$ / 348.31 g/mol

Yield: 0.38 g (41 %)

TLC: R_f = 0.61 (Aluminum oxide neutral, Hexane:EtOAc = 6:4)

mp.: decomposes

UV-Vis (ACN, c =1.5 · 10^{-5} mol · dm^{-3}): λ_{max} ~ 317 (18245) nm (ε / dm^3 ·mol^{-1} cm^{-1}).

2,7-Diamino-9-fluorenyl Phenyl Ether (Va)

The reduction of IVa to yield Va was identical to that of Vb and described previously. 0.36 g of IVa was dissolved in boiling 95% ethanol (100ml). The hot solution was mixed with 85% hydrazine hydrate (2.6 ml) and Raney nickel (35mg, wet weight), and heated on the oil bath for 30 min. After the addition of a second portion (2.6 ml) of hydrazine hydrate, the mixture was stirred and heated for another 30 min and filtered hot through celite. The progress of the reaction was monitored by TLC. The filtrate was concentrated, diluted with water, and the 2,7-diamino-9-fluorenol ether was collected by filtration. Crude product was purified by preparative chromatography with EtOAc as eluent to yield white amorphous powder.

Mol. formula/ Mol. Weight: $C_{19}H_{16}N_2O$ / 288.34 g/mol.

Yield: 0.19 mg (65 %)

TLC: R_f = 0.58 (Aluminum Oxide neutral, EtOAc).

mp.: 151-153 ºC

^{1}H NMR (400 MHz, *ACN*-d_3, *δ*/ ppm): δ 7.37 (m, 2H, *H5* and *H4*), δ 7.06 (dd, 2H, J=8.1Hz, J=14.5Hz, *H3'* and *H5'*), δ 6.95 (dd, 1H, J=3.2Hz, J=8.8Hz, *H4'*), δ 6.86 (d, 2H, J=8.6Hz, *H2'* and *H6'*), δ 6.68 (m, 2H, *H3* and *H6*), δ 6.59 (d, 2H, J=7.3Hz, *H1* and *H8*), δ 6.47 (s, 1H, *H9*) δ 4.05 (s, 4H, NH_2).

A representative spectrum is shown in Figure 7.

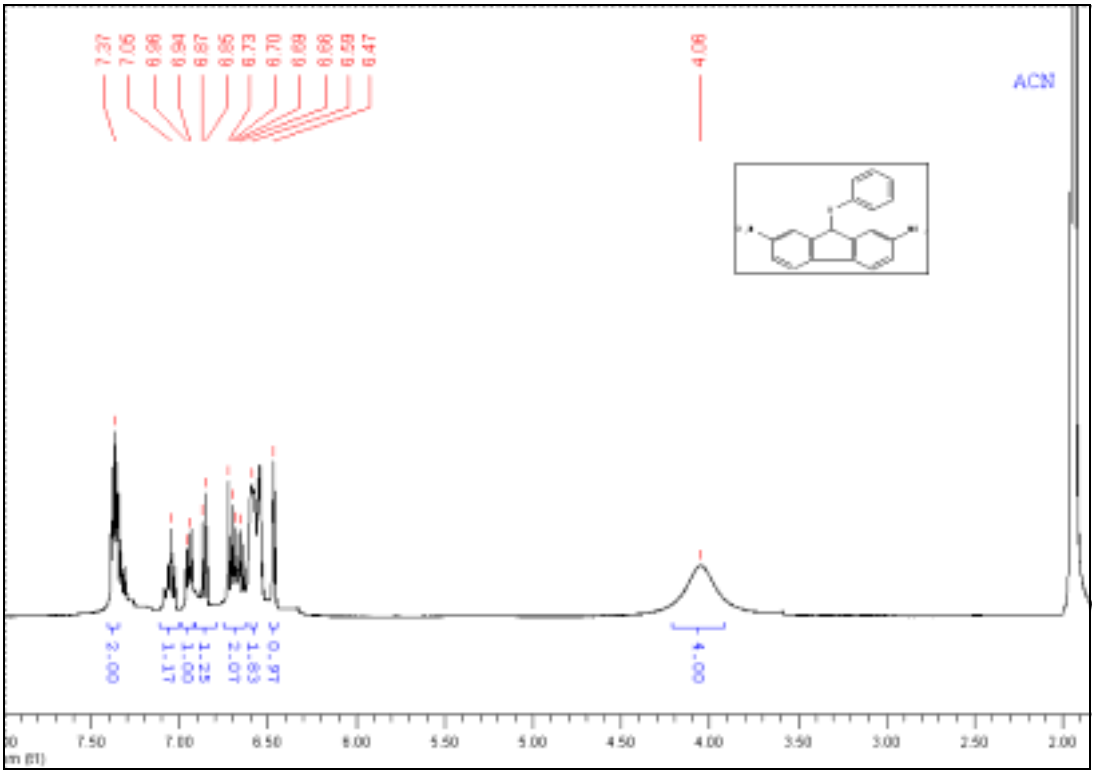

Figure 7. ^{1}H NMR spectrum (400 MHz, *δ*, *ACN*-d_3, 25°C) of 2,7-diamino-9-fluorenyl phenyl ether.

^{13}C NMR: We could not obtain good spectrum due to the poor solubility of 2,7-diamino-9-fluorenyl phenyl ether in the NMR solvents that were tried.

GC/MS ($(CH_3)_2CO$, *m/z*): M^+ 288, 270, 195, 135.

UV-Vis (H_2O, $c = 1.75 \cdot 10^{-5}$ mol $\cdot$ dm^{-3}): λ_{max} = 301 (14855) nm (ε / dm^3 ·mol^{-1} cm^{-1}).
UV-Vis (ACN, $c = 1.75 \cdot 10^{-5}$ mol $\cdot$ dm^{-3}): λ_{max} = 303 (17807) nm (ε / dm^3 ·mol^{-1} cm^{-1}).

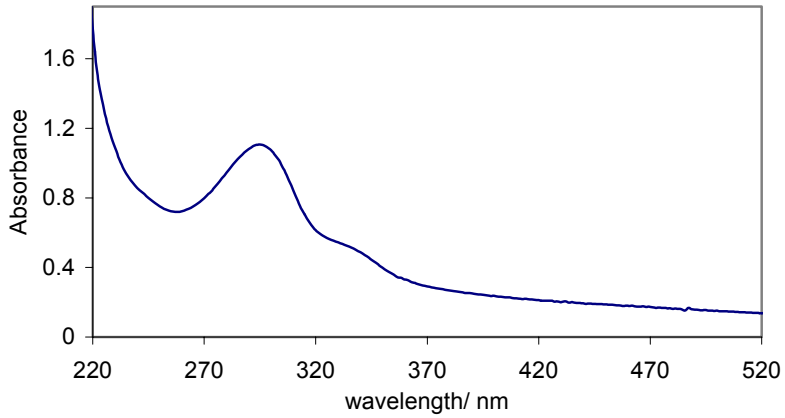

Figure 8. Absorption spectrum of 2,7-diamino-9-fluorenyl phenyl ether (λ_{max} = 301 nm) measured in water.

The methoxy-derivative of 2,7-diamino-9-fluorenol was of interest to us because it is expected as the main product of 2,7-diamino-9-fluorenol photolysis in methanol. Therefore, it can be obtained by direct photolysis of the parent compound or, alternatively, if one would want independent comparison, synthesized as proposed in Scheme 19. We have tried the first two steps but, due to many practical difficulties encountered and unfortunately not enough time, the synthesis have not been carried out until the very end.

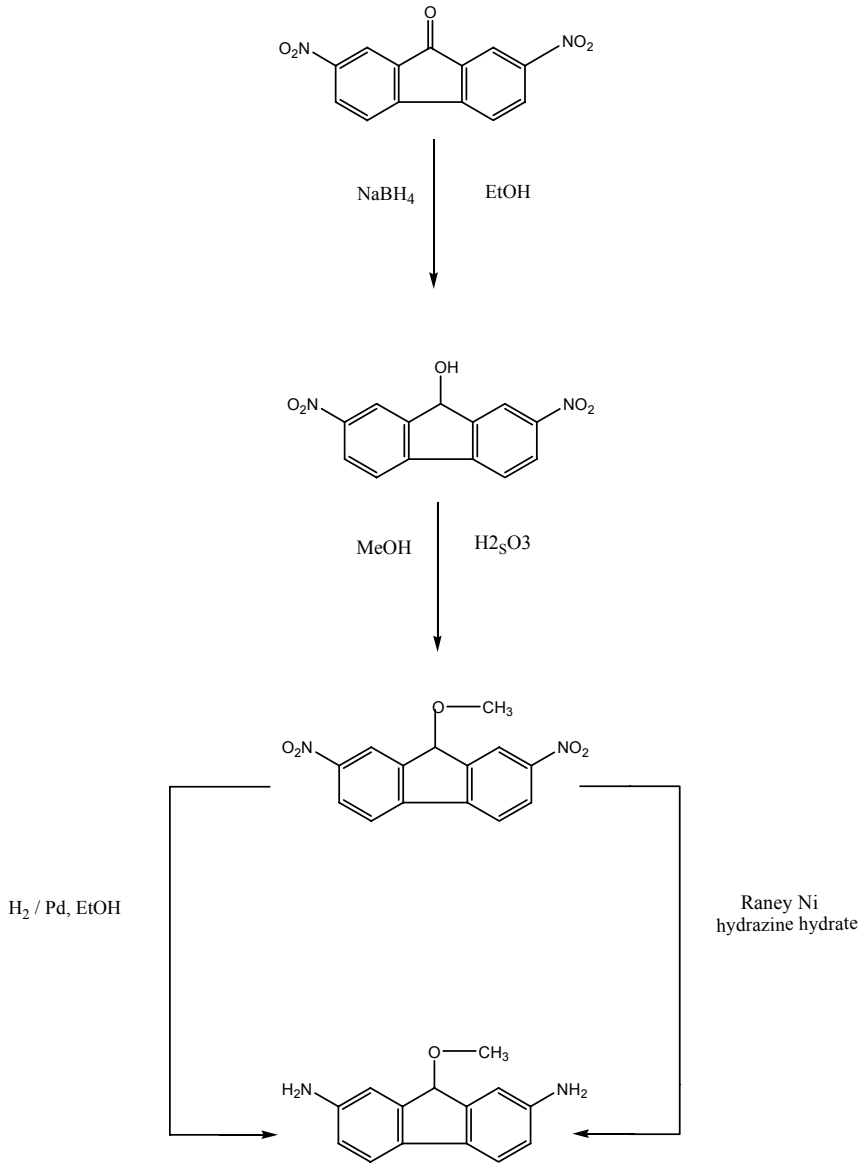

Scheme 19. Alternative synthesis of 2,7-diamino-9-methoxy-fluorenol.

4. Photochemical Studies

Product studies: UV-VIS spectroscopy, fluorescence spectroscopy or thin layer chromatography of the photolysis mixture were used to follow the progress of the irradiation and to identify some of the photoproducts. Thin-layer chromatography was performed on 5 x 10 cm neutral aluminum standard TLC plates from Merck, using either EtOAc : MeOH = 95:5 or EtOAc as a mobile phase, and observed under UV light of 254 nm. Fluorescence measurements were performed in methanol and excited at 290 nm. In several cases preparative irradiation of 4-6 mg of starting material was performed and photoproducts were isolated and identified by standard analytical techniques (NMR, GC-MS, MS).

Continuous irradiation: Solutions of 2,7-diamino-9-fluorenol, 2,7-diamino-9-fluorenyl acetate and 2,7-diamino-9-fluorenyl phenyl ether were irradiated with monochromatic light with a 125 W medium pressure Hg lamp filtered by a Pyrex glass sleeve (> 280 nm, > 313 nm) and stirred during the irradiation. The solutions were aerated. The progress of the photolysis was monitored by UV-VIS spectroscopy or thin layer chromatography. The experiments were performed in methanol or water in the case of 2,7-diamino-9-fluorenol and in water in the case of its derivatives.

Laser flash photolysis: Nanosecond flash photolysis studies were undertaken in order to understand the mechanism of the reaction. Experiments were performed with 1,1,1,3,3,3-hexafluoroisopropyl alcohol (HFIP), 2,2,2-trifluoroethanol (TFE), methanol and water solutions. They helped us identify transient intermediates and measure the rate constants of release of the protected substrate. The solutions were aerated unless specified otherwise, when samples were outgassed with consecutive freeze-pump-thaw cycles.

4.1. Photorelease from 2,7-diamino-9-fluorenol

4.1.1. Product studies

4.1.1.1. In polyfluorinated alcohols

Solutions of 2,7-diamino-9-fluorenol in 1,1,1,3,3,3-hexafluoroisopropyl alcohol (HFIP) and 2,2,2-trifluoroethanol (TFE) were irradiated by 308 nm laser and the products formed analyzed by UV-Visible spectroscopy.

The UV-Visible absorption spectra of 2,7-diamino-9-fluorenol in both HFIP and TFE show one maximum at around 300 nm. However, according to the absorption spectrum of the products, the photolysis afforded three new absorption bands, as shown in Figures 9 and 10. The first, with a broad maximum at around 444 nm, gave the irradiated solutions their characteristic yellow colour. The other two, with maxima at around 730 nm and 820 nm, fall into the infrared end of the spectrum and, since we suspected their cationic character, they have been far more interesting for us. The products lived over night in HFIP and at the minutes timescale in TFE. The absorption bands of the product are faster formed (only after 2 laser pulses) and of higher intensity in HFIP. However they are also well perceptible in TFE.

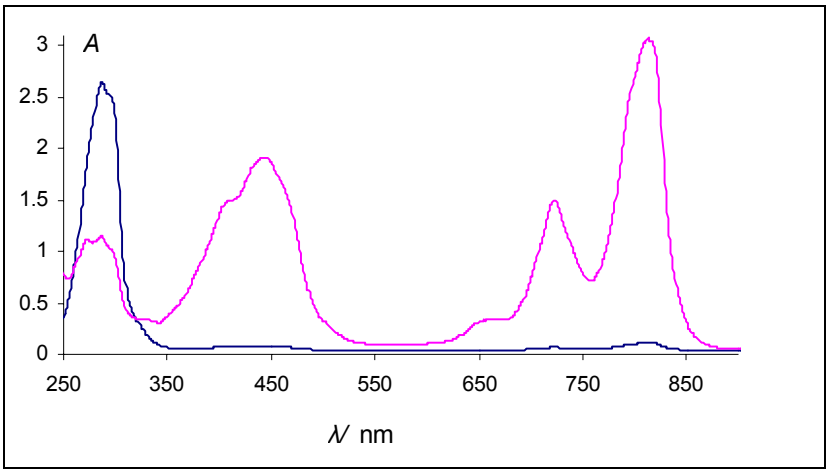

Figure 9. Absorption spectra of 2,7-diamino-9-fluorenol in HFIP measured before the laser flashes (blue curve) and after 10 laser flashes excited at 308 nm (pink curve).

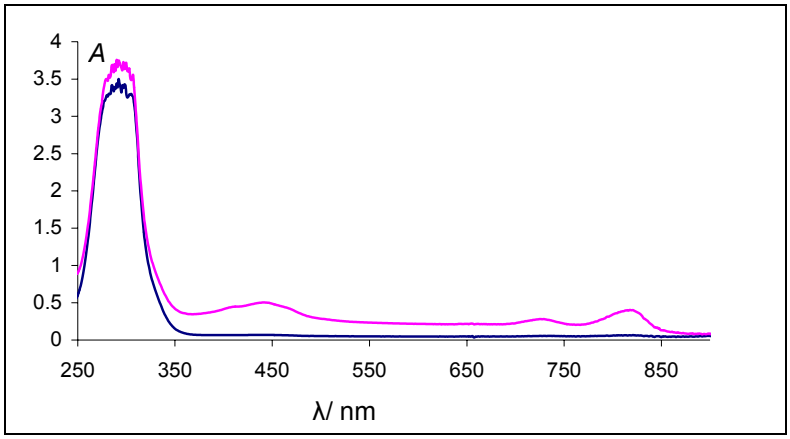

Figure 10. Absorption spectra of 2,7-diamino-9-fluorenol in TFE measured before the laser flashes (blue curve) and after 10 laser flashes excited at 308 nm (pink curve).

4.1.1.2. In methanol

Preparative photolyses in methanol were conducted in order to determine the photoproducts formed from 2,7-diamino-9-fluorenol. Based on Wan's work the main product expected was the methyl ether.

Wan and co-workers reported[51] that photolysis of 9-fluorenol in methanol and methanol-water mixtures leads to both homolytic and heterolytic cleavage via the excited singlet state. The partitioning between homolysis and heterolysis is controlled by the solvent composition. Both pathways, however, lead to the formation of 9-methoxyfluorene as the only observable product (Scheme 20).

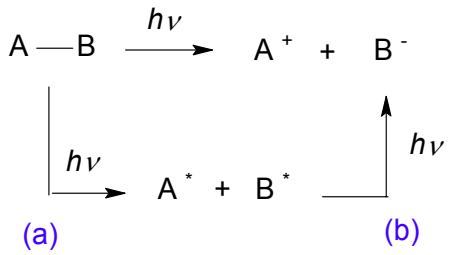

Scheme 20. Partitioning between homolysis and heterolysis of 9-fluorenol[51].

The authors postulated that 9-fluorenol (1) undergoes heterolytic bond cleavage upon excitation to yield a carbocation, which then reacts with methanol to yield the observed methyl ether (2), fluorene (3) and 9,9'-Bifluorene (4) were isolated after prolonged

irradiation of the reaction mixture. They were thought to form by photolysis of the primary photoproduct, the methyl ether (2), via homolytic cleavage of the C–O bond (eq 2). This is shown in the Scheme 21.

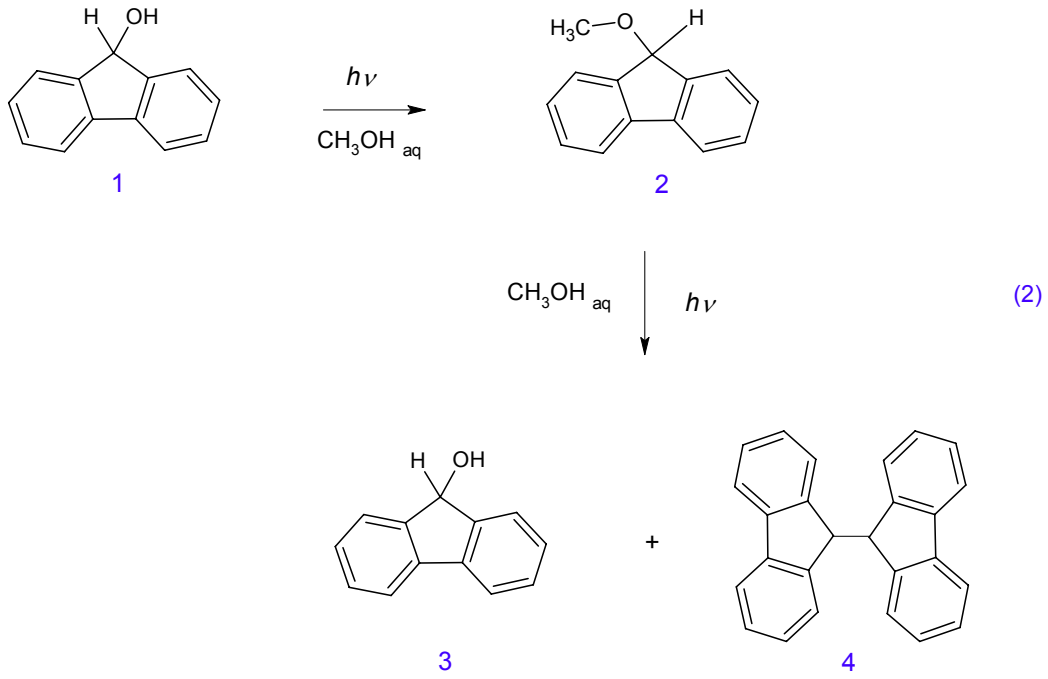

Scheme 21. Solvent dependent photolysis of 9-fluorenol.

We have analyzed photoproducts formed both in air-saturated and degassed solutions. A standard irradiation protocol was used: air saturated solutions of 2,7-diamino-9-fluorenol in methanol were continuously irradiated with a Hg lamp filtered by a Pyrex glass sleeve (> 280 nm). The irradiation was stopped after 4 or 20 h. The degassed solutions were photolyzed at 248 nm by using an excimer laser (10 flashes, sample shaken in between the flashes). Methanol was evaporated *in vacuo*. Thin layer chromatography, using EtOAc/MeOH = 95:5 as a mobile phase, showed that the products formed upon photolysis of 2,7-diamino-9-fluorenol could be well resolved. The crude product distribution was determined by GC/MS in acetone by comparison with the retention time of the authentic sample before the irradiation. Degassed samples irradiated by laser yielded the methoxy-derivative of 2,7-diamino-9-fluorenol as expected. (*m/z*) 226 (M^+), 196 (M^+–OCH_3). GC/MS spectra of the samples irradiated with a medium pressure Hg lamp yielded many different products which

were not all indentified. This indicated decomposition of the starting compound regardless of the time of irradiation. However, an intense M^+ peak of fluorene (*m/z*) 166 can be recognized on both the spectra recorded after 4 h and 20 h of irradiation.

This is in agreement with what is known that the main photoproduct of UV photolysis upon prolonged irradiation of 9-fluorenol (FOH) in non- and moderately polar solvents is fluorene[53]. In contrast to FOH, fluorene is a strongly fluorescing molecule with λ_{max} = 305 nm and it should be readily observed by its fluorescence emission.

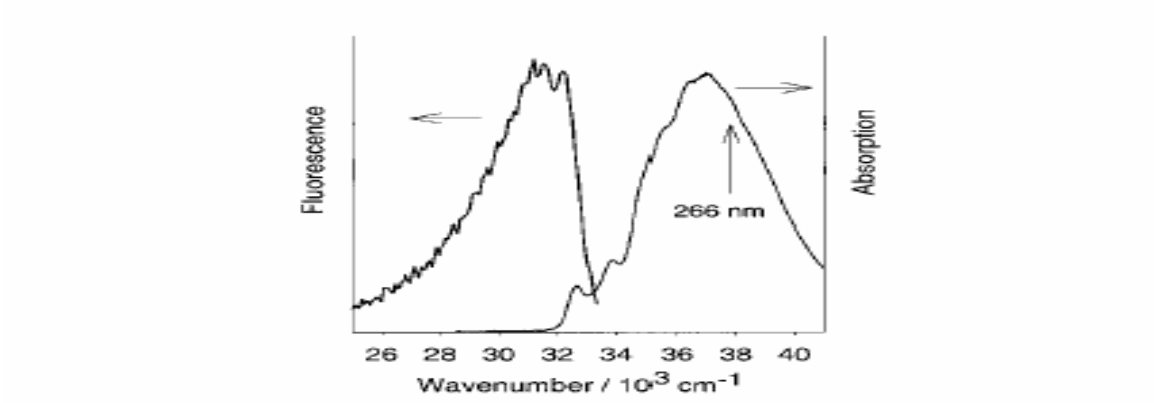

Figure 11. Fluorescence and absorption spectra of fluorene. [53]

Therefore we have done fluorescence measurements of 2,7-diamino-9-fluorenol solution in methanol before and after the photolysis. The same was repeated with 9-fluorenol to serve as a reference. According to the spectrum shown in Figure 12, there is fluorescence at 400 nm formed upon photolysis which we assigned to the 2,7-diaminofluorene. It is not as intense as that of fluorene.

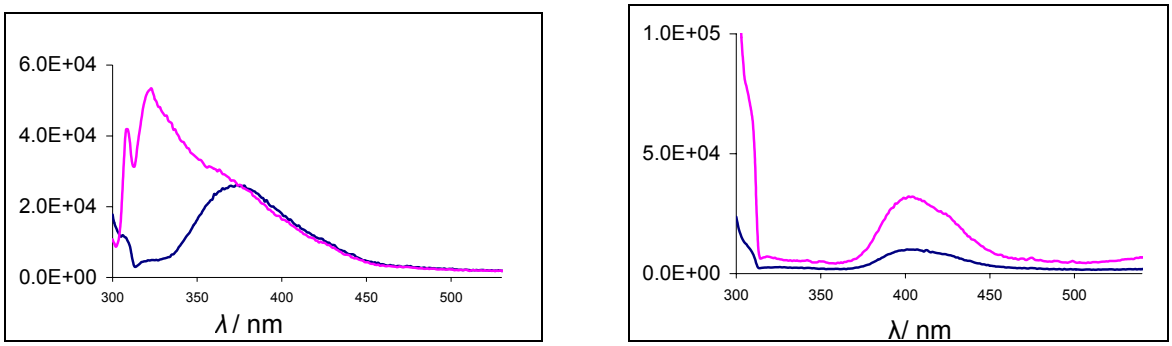

Figure 12. Fluorescence spectra of 9-fluorenol (left panel) and 2,7-diamino-9-fluorenol (right panel) in methanol, before (blue curve) and after photolyzing upon 248 nm laser pulse (pink curve), excited at 290 nm.

4.1.2. Laser Flash Photolysis

4.1.2.1. In polyfluorinated alcohols

Air saturated solutions of 2,7-diamino-9-fluorenol with an absorbance of 0.4 per cm (c=2.5 × 10^{-6} M) were excited at 308 nm to observe transient UV-Visible spectra and the kinetics of the transients. In order to obtain good transient absorption and kinetic traces in the infrared area, special settings to the standard laser set up was applied. For recording the transient absorption spectra the blaze angle in the spectrograph (angle between the grating normal and the groove normal) has been changed to allow the intensity of the diffracted light to be concentrated into a wavelength of 720 nm in order to observe the transients in the near infrared. RG 665 nm and RG 695 nm cut off filters have been used. Calibration of the x-axis of data was done by manually setting values against didymium reference. For recording the transient decay, instead of the standard Hamamatsu 1P28 photomultiplier tube (range of sensitivity 185–650 nm), 9785Q was used (range of sensitivity 300–800 nm) together with the RG 665 nm and RG 695 nm cut off filters.

The transient absorption spectrum both in TFE and HFIP showed the presence of three species. In TFE transients were observed at 420 nm, 772 nm and 862 nm, whereas in HFIP transients of a similar shape were slightly shifted to 420 nm, 765 nm and 826 nm. All of the transients are formed promptly after the laser pulse and shown in Figure 13. The transients are observed at times in microsecond regime. In the solvent TFE they have a lifetime of 6-8

μs. In HFIP they are much longer-lived, and still observed 30 μs after the laser pulse, which is consistent with what is already known. The lifetime of 9-fluorenyl cation in HFIP is reported to be 30 μs, and adding two amino groups in meta position is expected to make the cation even longer lived.

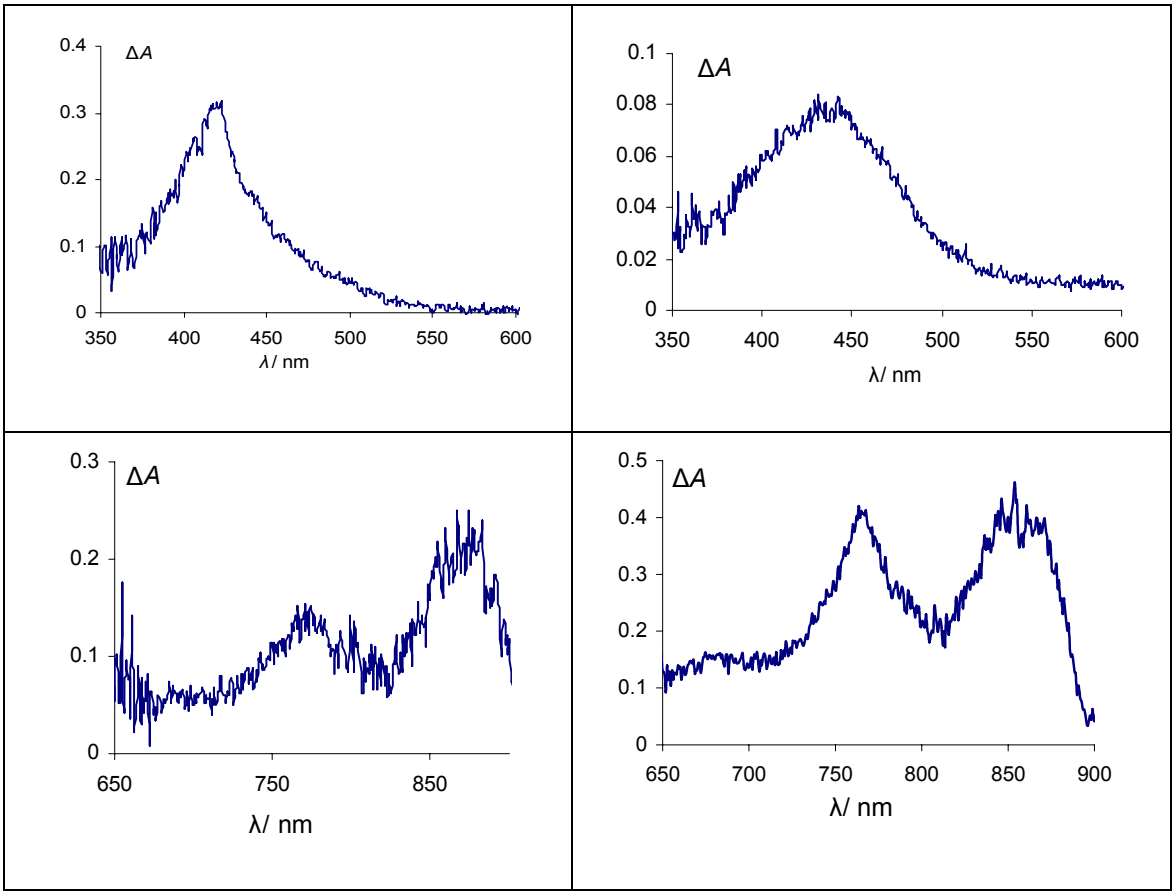

Figure 13. Transient absorption of 2,7-diamino-9-fluorenol in TFE (left panels) and HFIP (right panels), in the UV-Vis (above) and infrared area (below) of the spectrum, given in relative absorbance units, excited at 308 nm, $A_{308\ nm} = 0.4$ per cm, recorded just after the laser pulse.

Single wavelength kinetic traces in TFE (Figure 14) afforded the rate constants of the transient decay. They are summarized in Table 4. The decay obeys the first order rate law, with the residual absorbance observed for the band at λ_{max} of 420 nm. This could be assigned to product formation. We also observed that kinetic decay of the transient was getting slower with every additional laser shot, whereas the residual absorbance at 420 nm was getting

stronger. The growth of the signal is well resolved for the bands at 772 nm and 862 nm and will be discussed that later in this chapter.

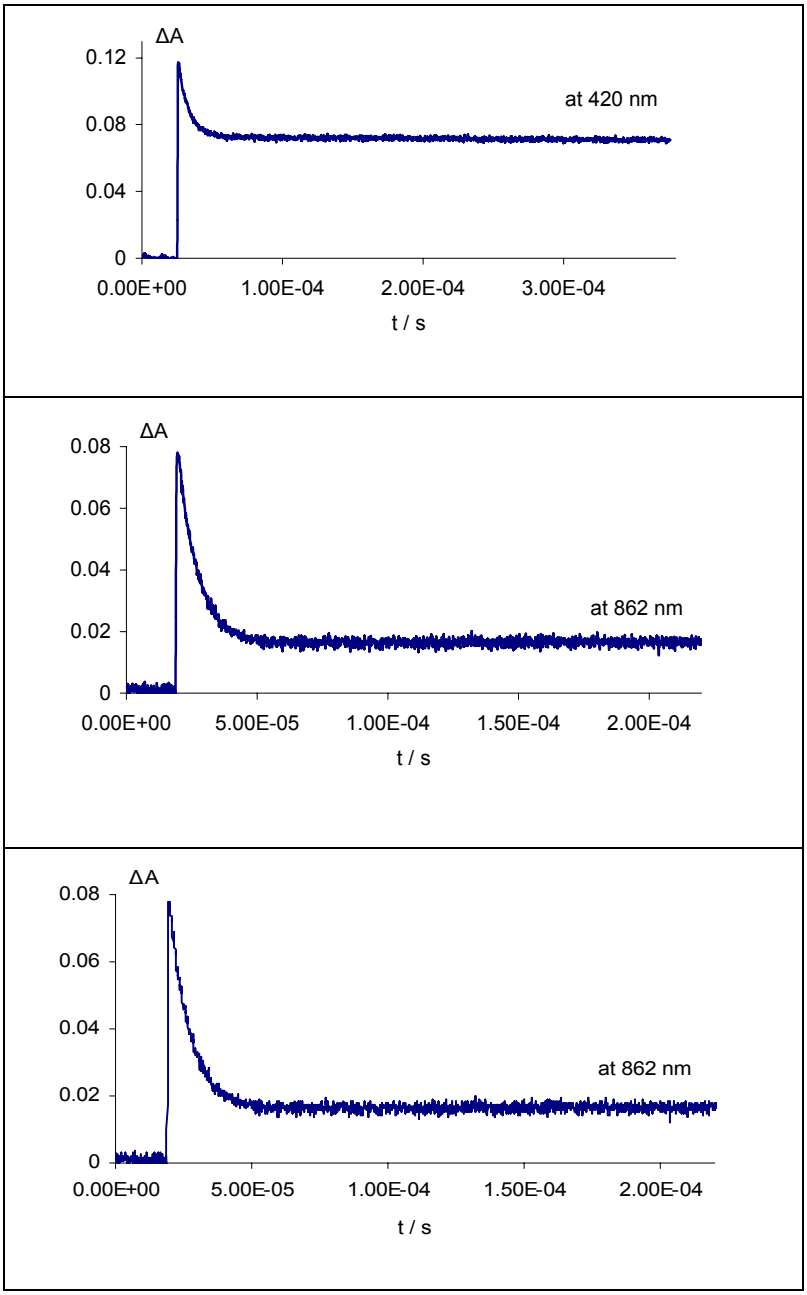

Figure 14. The decay kinetics of 2,7-diamino-9-fluorenol transient signals monitored in TFE, excited at 308 nm, $A_{308\ nm} = 0.4$ per cm, c=2.5 × 10^{-6} M.

Rate constants in TFE, s^{-1}		
at 420	at 772 nm	at 862 nm
$(1.17 \pm 0.01) \times 10^5$	$(1.57 \pm 0.01) \times 10^5$	$(1.31 \pm 0.01) \times 10^5$
	$(4.45 \pm 0.03) \times 10^6$	$(3.71 \pm 0.32) \times 10^6$

Table 4. Rate constants at 20 ºC for the decay of 2,7-diamino-9-fluorenol transients in TFE, excited at 308 nm, $A_{308\ nm} = 0.4$ per cm.

It is evident that the decay of the 862 nm band is slightly slower in regard to 772 nm band decay.

Transients in the infrared area: an unusual case

Transients in the infrared area were of special interest as they have not been reported before. Therefore, our attention was drawn to them. Assuming that they are of the same type in the solvents TFE and HFIP, and taking in account cost effectiveness, we have chosen to study 2,7-diamino-9-fluorenol transients in the solvent TFE rather than in costly HFIP. In order to determine whether they are of cationic character, we have studied TFE / water and TFE / NaOH systems, as well as oxygen-saturated and degassed samples. Nucleophiles, such as water, should accelerate the transient decay of a cation, whereas oxygen should have no influence.

Therefore, in our first experiment 2,7-diamino-9-fluorenol was photolyzed in pure TFE, and then in TFE with different amounts of water added, pure water and finally with 5 or 10 % sodium hydroxide added to a water solution. Kinetics was recorded at 420 nm, 772 nm and 862 nm. Upon the photolysis of 2,7-diamino-9-fluorenol in this system, the kinetic traces obtained showed both rise and decay of the signal. Table 5 summarizes decay constants (k_2) and Table 6 growth constants (k_1).

Solvent	Decay constant, k_2 (10^5 s^{-1}) at 420 nm	at 772 nm	at 862 nm
TFE only	1.17 ± 0.01	1.57 ± 0.01	1.31 ± 0.01
10% water	2.67 ± 0.02	3.00 ± 0.01	2.66 ± 0.01
20% water	3.49 ± 0.18	4.68 ± 0.01	4.55 ± 0.02
40% water	5.82 ± 0.03	5.06 ± 0.02	5.32 ± 0.04
70% water	6.93 ± 0.03	7.22 ± 0.02	8.04 ± 0.28
all water	1.27 ± 0.02	2.09 ± 0.05	1.96 ± 0.06
5% NaOH	1.55 ± 0.02	1.64 ± 0.02	not observed
10% NaOH	1.42 ± 0.03	1.80 ± 0.02	not observed

Table 5. Rate constants at 20 ºC for the decay of 2,7-diamino-9-fluorenol transient in TFE containing water and strong base, at different wavelengths, excited at 308 nm, $A_{308\ nm} = 0.4$ per cm.

Table 5 shows that the addition of either water or a strong base, namely sodium hydroxide, does accelerate the decay of the transient. However, we have expected this effect to be much more pronounced. In pure water the rates fail to follow this pattern. Our spectra show that all three bands (λ_{max} of 420 nm, 772 nm and 862 nm) formed upon photolysis under the same conditions (in TFE as a solvent, adding the same amount of water and using the same cut off filters) decay with similar kinetics and therefore should represent the same intermediate. However, it is a bit surprising that is difficult to obtain a good kinetic trace for the transient at 862 nm in case of a strong base added. The decay obeys the first order rate law, with the residual absorbance observed for the band at λ_{max} of 420 nm. This could be assigned to product formation.

The growth of the signal is well resolved for the bands at 772 nm and 862 nm. This growth is tentatively assigned to a triplet intermediate. With addition of water to the TFE solution, the rise of the signal is getting slower, as shown in the Table 6. Comparing the kinetics of the two bands, the transient at 772 nm forms faster regardless of the amount of water added.

Solvent	Growth constant, k_1 (10^6 s^{-1}) at 772 nm	at 862 nm
TFE only	4.45 ± 0.03	3.71 ± 0.32
10% water	3.37 ± 0.03	2.49 ± 0.04
20% water	3.21 ± 0.02	1.92 ± 0.04
70% water	1.99 ± 0.02	1.46 ± 0.07
5% NaOH	2.07 ± 0.05	not observed
10% NaOH	2.27 ± 0.22	not observed

Table 6. Rate constants at 20 ºC for the rise of 2,7-diamino-9-fluorenol transient in TFE containing water and strong base, at different wavelengths, excited at 308 nm, $A_{308\ nm}$ = 0.4 per cm.

In order to confirm the acceleration of transient decay with added nucleophile, we also recorded the absorbance spectra, in the same solvent system, at different time delays after the laser pulse, namely after 800 ns and 3 μs. Solutions were excited with 308 nm laser pulse, $A_{308\ nm}$ = 0.4 per cm.

Solvent	Intensity of the transient absorbance (ΔA) at 772 nm		at 862 nm	
	800 ns after	3 μs after	800 ns after	3 μs after
TFE only	0.16	0.11	0.14	0.15
5% water	0.22	0.15	0.20	0.17
10% water	0.22	0.10	0.21	0.11
20% water	0.14	0.10	0.12	0.11
40% water	0.16	0.05	0.14	0.05
5% NaOH	0.09	0.06	0.08	0.06

Table 7. Dependence of the intensity of the transient absorbance of 2,7-diamino-9-fluorenol in TFE (given in relative absorbance units) on the amount of water/strong base added, recorded at two different wavelengths and

at two different delays after the laser pulse, with 300 ns and 1μs gate pulse width (the length of time that intensifier tube is switched/gated on) respectively.

This as well allowed to establish whether the position of the absorbance maximum of the transient intermediate changes with time.

The results summarized in Table 7 are consistent with the results already obtained from the kinetic traces. The addition of strong base quenches the transient absorption to some extent, though it is still surprising it does not do it more efficiently. The addition of water appears to intensify the transient absorption at first, but, with adding greater amounts, the intensity of the transient absorption decreases again. This could be related to small amounts of water present in TFE. However, it is certain that the position of the transient absorption does not change either with the time or with the addition of water. It is also evident that the band at 772 nm is slightly more intense than the one at 862 nm but of a similar shape. The spectra obtained under the same conditions in pure water as a solvent showed no transients in the red area both at very early times after the laser pulse and on the microsecond scale.

There are two comments regarding the kinetics of parent 9-fluorenol compound reported in literature. (i) At high laser doses the decay becomes faster, by as much as 50% at a dose of 80 mJ as compared to 3 mJ.[50] Moreover, there are slight deviations of the fit of the experimental data from the exponential rate law, unlike the situation at low laser intensities where excellent fits are obtained. This is attributed to the presence of an anion which must accompany the formation of the cation in the photoheterolysis. This anion is initially hydroxide, but this should be rapidly neutralized by TFE to generate the corresponding alkoxide ion. It is suspected that at higher laser doses some fraction of the cation reacts with this anion, and thus the decay is faster. Moreover since this anion is present at all times in equal concentration as the cation this combination will follow second-order kinetics. (ii) An increase of the decay was also observed at higher concentrations of the precursor 9-fluorenol.[54] This can be attributed to a reaction of the cation with the excess 2,7-diamino-9-fluorenol present after photolysis. A plot of rate constant versus concentration of 9-fluorenol is reasonably linear, giving a second-order rate constant of 5×10^6 M^{-1} s^{-1}. A simple interpretation is that this reaction involves reacting with the alcohol group of 9-fluorenol.

In order to establish whether oxygen influences the kinetics of 2,7-diamino-9-fluorenol transient in the solvent TFE, 2,7-diamino-9-fluorenol was photolyzed both in air saturated and degassed solution, and the constant of transient decay was measured.

	Decay constant, k_1 (10^5 s^{-1})	
	at 772 nm	at 862 nm
degassed sample	0.80 ± 0.01	0.82 ± 0.01
not degassed sample	1.43 ± 0.01	1.42 ± 0.01

Table 8. Dependence of the rate constant of 2,7-diamino-9-fluorenol decay in TFE on the oxygen, excited at 308 nm, $A_{308\ nm} = 0.4$ per cm.

Table 8 demonstrates that the rate constant of the transient decay in absence of oxygen is slightly slower, therefore the transient longer lived in absence of oxygen. This is to be expected for a triplet but not a cation. However, the decay is not terribly dependant on oxygen. A possible explanation for a small difference in the speed of the decay is exposing degassed solution to extreme temperatures in the process of degassing. This possibility was ruled out by performing the same experiment by photolysing first the degassed solution, and then obtaining the aerated solution by blowing oxygen through it for ~ 5 minutes and measuring the rate of photolysis in this manner aerated solution. In this way both of the samples have been exposed to the same conditions. Purging the degassed solution with oxygen made the decay of the transient faster than in the initial degassed solution, as shown in Table 9.

.	Decay constant, k_1 (10^5 s^{-1})	
	at 772 nm	at 862 nm
degassed sample	0.81 ± 0.01	0.62 ± 0.01
oxygenated sample	2.86 ± 0.01	2.46 ± 0.01

Table 9. Dependence of the rate constant of 2,7-diamino-9-fluorenol decay in TFE on the oxygen, excited at 308 nm, $A_{308\ nm} = 0.4$ per cm.

Comparing Tables 8 and 9, it is obvious that the speed of the transient decay is in order: oxygenated sample > degassed sample > not degassed sample. Therefore, we conclude that oxygen does have accelerating effect on the decay of the transient intermediate.

Attempt to determine whether the transient observed at 772 nm and 862 nm is a cation, radical or that of a mixed character has been made by trying to generate the 2,7-diamino-9-flyorenyl radical ($F^{\bullet}$) and record its absorption spectrum. Our idea to do this was by photolyzing di-*tert*-butyl peroxide (DTBP) in the presence of high concentration of 2,7-diamino-9-fluorenol by 351 nm laser pulse. DTBP flash photolysis yields *tert*-butoxy radicals which rapidly abstract hydrogen from hydrocarbons, ethers and alcohols to give carbon-centered radicals. At the same time DTBP is an efficient triplet quencher so the triplet-triplet absorptions of the amines do not interfere. In order to determine the exact concentration of the compound required for the radical reaction to occur, preliminary experiments have been successfully done with aniline and fluorene. The same reaction was repeated with 2,7-diamino-9-fluorenol. However, no transients of the 2,7-diamino-9-fluorenol have been observed. Few explanations are plausible. It could be either due to the low concentration of diaminofluorenol in DTBP (10^{-3} M), air-saturation of the sample or the radical is simply too short lived to be observed with our equipment.

In order to determine whether the photoproduct of 2,7-diamino-9-fluorenol irradiated in TFE is formed via a singlet or triplet state, quenching experiments were done. Naphthalene ($E_T \approx$ 253 kJ/mol[70]) was used as the triplet quencher for the photoreaction of 2,7-diamino-9-fluorenol occurring upon the excitation at 308 nm in TFE. Concentration of naphthalene was 10^{-4} M. The samples have been excited with 351 nm laser pulse. These experiments still yielded photoproduct strongly absorbing at 728 nm and 819 nm, as shown in Figure 16. The intensity of the absorption remains unchanged in regard to that of the photoproduct formed in the absence of the quencher. There are few plausible explanations. The product is either formed via singlet state or via very fast triplet which cannot be quenched by naphthalene.

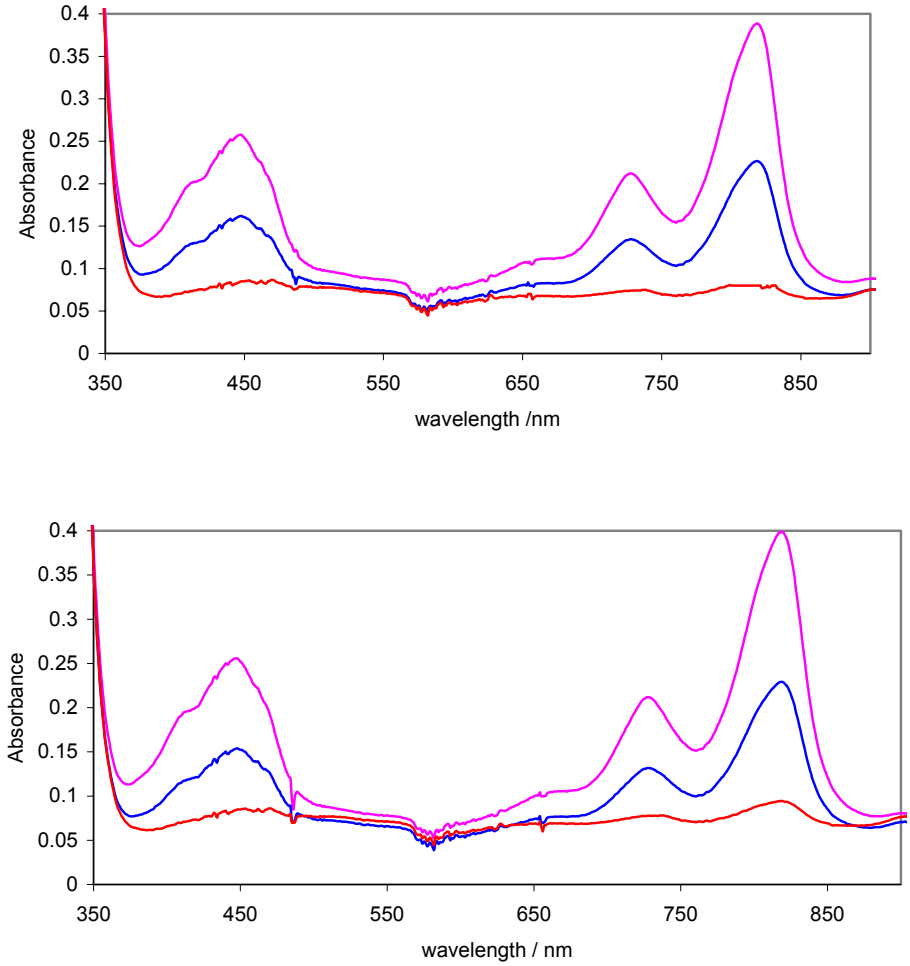

Figure 16. Absorption spectra of 2,7-diamino-9-fluorenol in TFE measured before the laser flashes (red curve), after 1 laser flash (blue curve) and after 3 laser flashes (pink curve) excited at 351 nm, without the quencher (above) and in the presence of naphthalene (below). $A_{351\ nm} = 0.3$ per cm.

4.1.2.2. In methanol and water

Laser flash photolysis of 2,7-diamino-9-fluorenol in methanol gave a strong transient signal in the range of 390 nm to 450 nm, λ_{max}=420 nm. In water we obtained signal of similar shape in the same range. The only difference was slight blue shift of the maximum, λ_{max} ~ 405 nm (Figure 17). In both solvents the transient absorption was formed within the duration of the laser pulse (ca. 25 ns). No transients in the infrared area were observed. Transient spectra taken in methanol at longer delay times after the laser flash proved that the strong absorption is still stable after 16 μs.

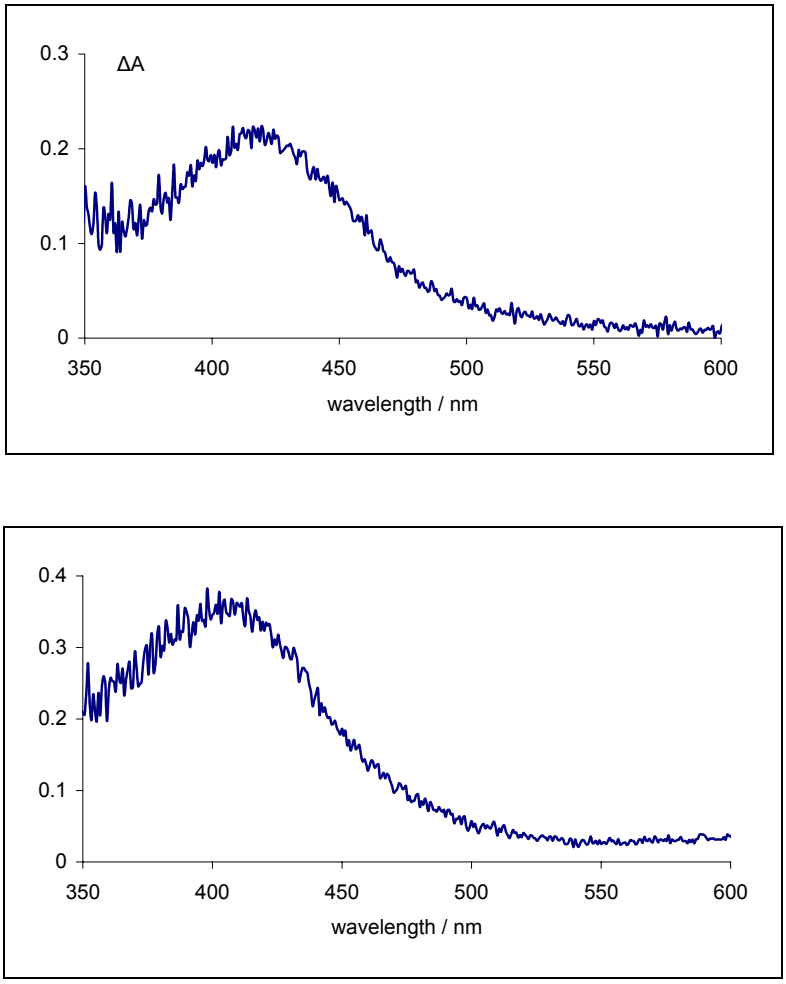

Figure 17. Transient absorption of 2,7-diamino-9-fluorenol (given in relative absorbance units) in methanol (above) and water (below), excited at 308 nm, $A_{308\ nm} = 0.4$ per cm, recorded just after the laser pulse.

A kinetic trace recorded at 420 nm in methanol and at 405 nm in water solution is shown in Figure 18. Kinetic analysis by a least-squares procedure showed that the transient in methanol decays by first order kinetics with a rate constant of (3. 15 ± 0.02) x 10^5 s^{-1}, but does not return to baseline on the microsecond timescale. The end absorption is assigned to a product formation. In water, the kinetic curves were best fitted with combination of two exponents, suggesting a parallel decay of two species with similar absorption spectra, and were (1.10 ± 0.01) x 10^5 s^{-1} and (1.23 ± 0.02) x 10^4 s^{-1}. No residual absorbance was detected.

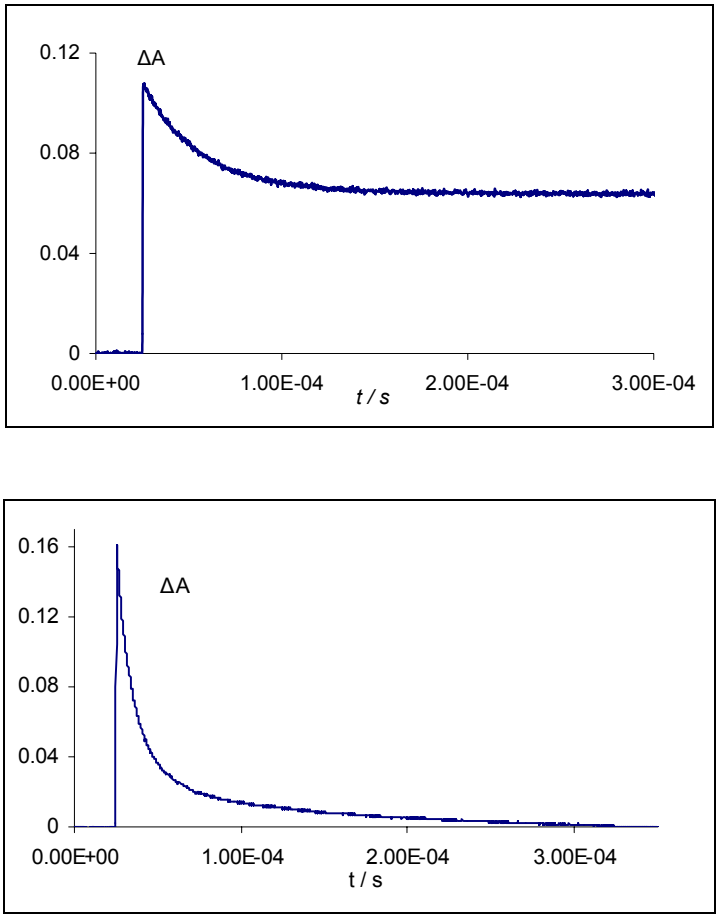

Figure 18. The decay kinetics monitored in a solution of 2,7-diamino-9-fluorenol in methanol at 420 nm (above) and in water at 405 nm (below) , excited at 308 nm, $A_{308\ nm} = 0.4$ per cm, c=2.5 × 10^{-6} M.

4.1.3. Discussion

Taking in account the fact that 2,7-diamino-9-fluorenol exhibits quite different behavior upon photolysis in polyfluorinated alcohols and, on the other hand, in methanol and water, those two cases will be addressed on an individual basis.

In polyfluorinated alcohols:

UV-Visible monitoring of the photoreaction revealed three new absorption bands formed. Two of them, with maxima at around 730 nm and 820 nm, fall into the infrared end of the spectra and have been of special interest to us as they have not been observed in the case of

9-fluorenol. The transient absorption spectrum upon the laser flash photolysis both in TFE and HFIP showed the presence of three species. In TFE transients were observed at 420 nm, 772 nm and 862 nm, whereas in HFIP transients of a similar shape were slightly shifted and found at 420 nm, 765 nm and 826 nm. All of the transients are formed promptly within the laser pulse. The band at 772 nm is slightly more intensive than the one at 862 nm but of a similar shape. The fact that they are about 40 nm blue-shifted in regard to the absorption bands of the transient observed upon photolysis lead us to the conclusion that there are four different species forming, two transients and two products.

The position of the transient absorption does not change either with time or with the addition of nucleophile.

Kinetic traces obtained showed that the decay of all three bands obeys the first order rate law, with the residual absorbance observed for the band at λ_{max} of 420 nm only. This is assigned to product formation. The growth of the signal is well resolved for the bands at 772 nm and 862 nm. This growth is tentatively assigned to a triplet intermediate and comparing the kinetics of the two bands it is clear that the transient at 772 nm forms faster. However, quenching experiments with naphthalene indicate that the reactive state involved in the photolysis of 2,7-diamino-9-fluorenol is either a singlet state or a very fast triplet. A transient observed is moderately oxygen sensitive (accelerating effect on the decay).

The addition of either water or a strong base to the TFE solution accelerates the decay of the transient, therefore its cationic character can be assumed. This is in agreement with findings reported in literature for the parent compound 9-fluorenol. We have expected this accelerating effect to be more pronounced.

In methanol and water:

GC/MS monitoring of the photoreaction in methanol in the case of the degassed samples showed that the methoxy-derivative of 2,7-diamino-9-fluorenol is formed. The photolytic conversion was clean and uniform process. The air saturated samples upon irradiation yielded many different products which were not all identified. This indicated decomposition of the starting compound regardless of the time of irradiation. However, an intensive M^+ peak fluorene can clearly be recognized on the GC/MS spectra. The fluorescence measurements confirmed the same. This supports findings of Wan and co-workers who

postulated that 9-fluorenol forms fluorene upon prolonged irradiation. This experiment did not allow for determination of the rate of conversion and the quantum yield.

Laser flash photolysis showed only one transient at 420 nm. Unlike in the case of polyfluorinated alcohols, the spectra obtained in methanol and pure water showed no transients in the red area both at very early times after the laser pulse and on the microsecond scale. The transient intermediate in methanol solution decays with the rate constant of (3. 15 $\pm$ 1.17) x 10^5 s^{-1}, whereas single wavelength kinetic traces in water solution show byexponential decay with rate constants of (1.10 $\pm$ 0.01) x 10^5 s^{-1} and (1.23 $\pm$ 0.02) x 10^4 s^{-1}. The end absorption detected upon photolysis in methanol was assigned to a product formation.

4.2. Photorelease from 2,7-diamino-9-fluorenyl acetate

In order to assess whether it would be possible to efficiently release acetic acid from 2,7-diamino-9-fluorenyl acetate, we investigated 2,7-diamino-9-fluorenyl acetate in aqueous solution. The reaction was expected to lead to the formation of 2,7-diamino-9-fluorenol, as shown in Scheme 22.

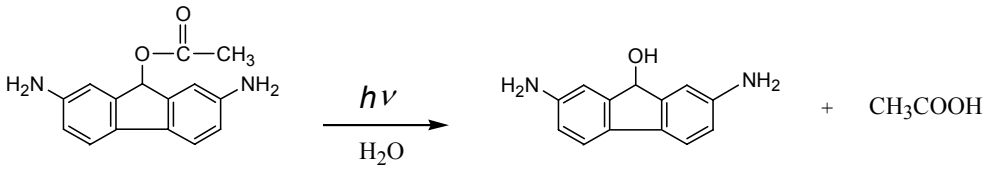

Scheme 22. Elimination of CH_3COOH from 2,7-diamino-9-fluorenyl acetate.

4.2.1. Product studies

Solutions of 2,7-diamino-9-fluorenyl acetate in water were photolyzed at 308 nm and 351 nm with 10 and 20 laser flashes.

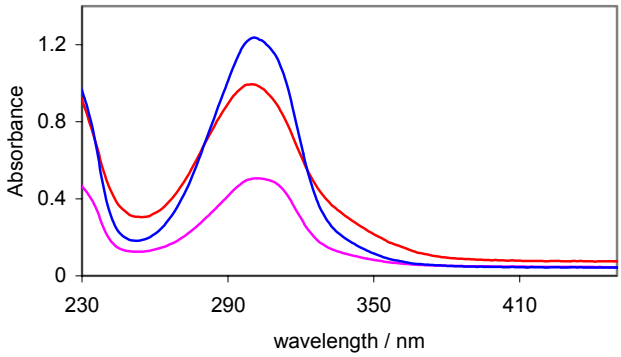

Figure 19. Overlapping absorption of 2,7-diamino-9-fluorenol and its acetate derivative (λ_{max} = 301 nm): 2,7-diamino-9-fluorenol (pink), 2,7-diamino-9-fluorenyl acetate measured before the laser flashes (blue) and 2,7-diamino-9-fluorenyl acetate after 20 laser flashes excited at 308 nm (red). Measured in water.

The progress of the reaction could not be monitored by UV-VIS spectroscopy because of the overlapping absorption of 2,7-diamino-9-fluorenyl acetate and newly formed 2,7-diamino-9-fluorenol, both absorbing at ~ 302 nm (Figure 19). Also, the concentration of the solutions was too low (c= 1.75 $\cdot 10^{-5}$ M) to allow for direct follow-up by thin layer chromatography or GC/MS. This unabled us to quantitively measure the conversion.

However, once the irradiation was stopped and the solvent evaporated, the product distribution was established by thin layer chromatography using EtOAc as mobile phase and neutral aluminum as stationery one. A new, weak spot appeared. Comparing the retardation factor (R_F) for 2,7-diamino-9-fluorenyl acetate, photolysis mixture and independently synthesized 2,7-diamino-9-fluorenol, it is evident that the final product of the photolysis is 2,7-diamino-9-fluorenol, as expected (Figure 20). Thin layer analysis did not reveal any dependence of the product distribution neither on the irradiation wavelength nor on the number of flashes. The new spot assigned to the product appears promptly after the irradiation, therefore we are quite confident that the acetate is a good leaving group for this system.

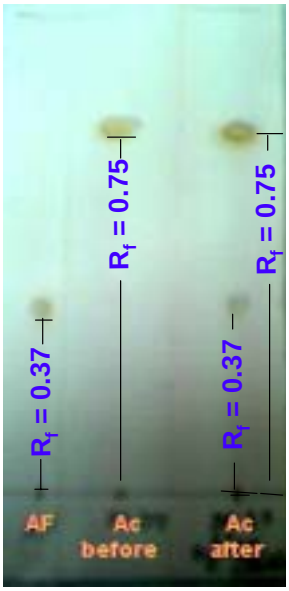

Figure 20. Raw, uncorrected image of TLC plate showing 2,7-diamino-9-fluorenol (AF), 2,7-diamino-9-fluorenyl acetate before irradiation (Ac before) and 2,7-diamino-9-fluorenyl acetate after 10 flashes at 308 nm laser (Ac after), using neutral aluminum as stationery phase and EtOAc as mobile one.

The product distribution established by thin layer chromatography was confirmed by GC/MS. After the irradiation was stopped and solvent evaporated, GC/MS spectrum was

recorded in acetone and the photolyzed mixture consisted of 2,7-diamino-9-fluorenyl acetate, 2,7-diamino-9-fluorenol and 2,7-diaminofluorene.

Attempts have been made to titrate the free acetic acid released upon the irradiation of 2,7-diamino-9-fluorenol in order to quantitatively determine the amount of the protected substrate liberated, being important characteristic of a photoremovable protecting group. A $2 \cdot 10^{-3}$ M aqueous solution of 2,7-diamino-9-fluorenol was photolyzed with a medium pressure Hg lamp using 313 nm filter. The progress of the reaction was followed by measuring the pH of irradiated solution. After the reaction was stopped, the solution was titrated with 0.02 ml of 0.4 M sodium hydroxide, adding 0.001 ml at the time. However, the results were inconclusive. The pH value of the irradiated solution did not drop down to ~ 4.8 as expected in the case of release of the acetic acid, regardless the time of irradiation. It reached the value of ~ 5.5 during the prolonged irradiation and then decomposed. This could be explained by possible formation a buffer due to the amino functions present.

4.2.2. Discussion

An important issue when dealing with phototriggers is the rate of release of the caged substrate. Our irradiation experiments did not allow us to measure directly the rate of release, because of the overlapping absorption of the starting compound and the product. Due to the small amount of pure compound obtained as well as its poor solubility, difficulties have been encountered in product analysis of the photolyzed mixture. However, based on the thin layer chromatography and GC/MS, we are quite confident that the photoreaction leads to efficient release of acetic acid.

4.3. Photorelease from 2,7-diamino-9-fluorenyl phenyl ether

2,7-diamino-9-fluorenyl phenyl ether is expected to photorelease phenol with formation of 2,7-diamino-9-fluorenol upon irradiation in water, as shown in Scheme 23.

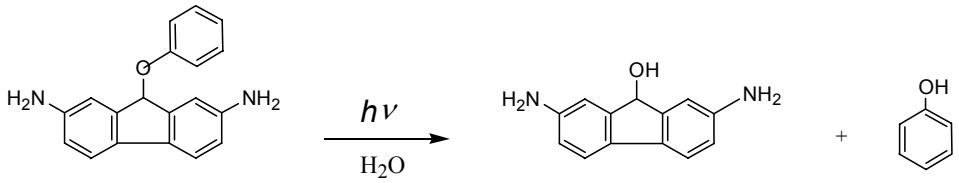

Scheme 23. Elimination of phenol from 2,7-diamino-9-fluorenyl phenyl ether.

4.3.1. Product studies

Solutions of 2,7-diamino-9-fluorenyl phenyl ether in water were irradiated at 308 nm and 351 nm with 10 or 20 laser flashes.

Similar to the acetate derivative, it was not possible for the progress of the reaction to be monitored by UV-VIS spectroscopy due to the lack of a qualitative change in the absorption of the starting material and the product, both absorbing at ~ 301 nm. In addition, the absorption of released phenol was 'masked' by that one of 2,7-diamino-9-fluorenol and 2,7-diamino-9-fluorenyl phenyl ether.

Therefore we decided to study the same system in a basic aqueous solution (pH = 12.5). Initially we expected to see a new absorption band from the released phenolate but the overlap with the broad maximum of fluorenyl compounds still did not allow for detecting it (Table 10).

	λ_{max} / nm, pH=7	λ_{max} / nm, pH=12.5
phenol	270	285
2,7-diamino-9-fluorenyl phenyl ether	270 – 330 (301)	270 – 330 (295)

Table 10. Absorption maxima for phenol and area where 2,7-diamino-9-flurenyl ether absorbs (with the absorption maximum given in brackets), in neutral and basic water solutions.

Furthermore, the absorption of 2,7-diamino-9-fluorenyl phenyl at 295 nm was not increasing. Instead, a broad band with a maximum at ~ 450 nm was formed that indicating the decomposition of the released substrate. This is in agreement with phenolate decomposing upon irradiation. The irradiation wavelength did not have any effect on the photolysis. The same results were obtained upon continuous irradiation at the mercury lamp and using 313 nm cut off filter. The corresponding absorption spectra are shown in Figures 21 and 22.

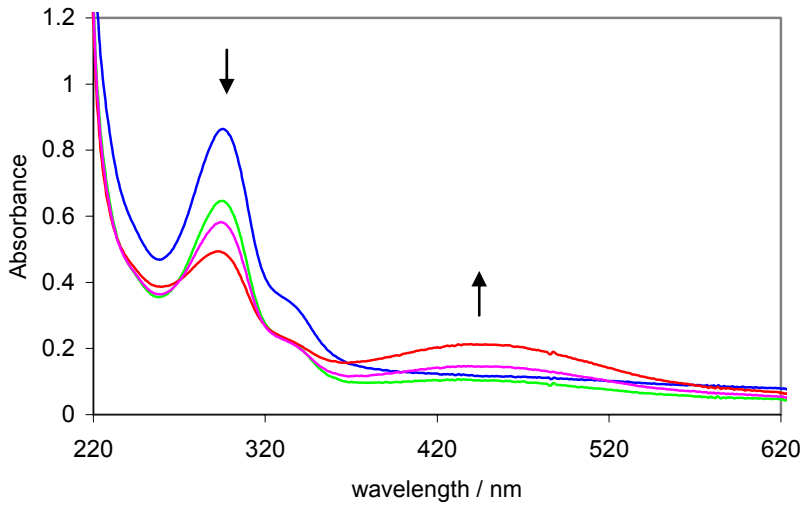

Figure 21. 2,7-diamino-9-fluorenyl phenyl ether absorption spectrum in basic water solution (pH=12.5) (blue curve), after 5 flashes (green), after 10 flashes (pink) and after 20 flashes (red curve) irradiated at 308 nm laser. Black arrows indicate the change of the absorption during the irradiation period.

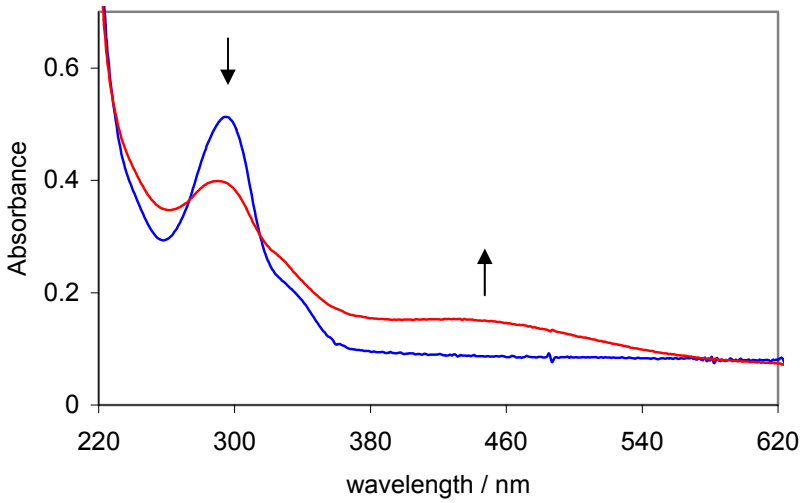

Figure 22. 2,7-diamino-9-fluorenyl phenyl ether before (blue curve) and after (red curve) the irradiation for 3.5 hrs in basic water solution (pH=12.5) with the 313 nm cut off filter. Black arrows indicate the change of the absorption during the irradiation period.

We have attempted to follow 2,7-diamino-9-fluorenyl phenyl ether photolysis in water by NMR. 5.2 mg of 2,7-diamino-9-fluorenyl phenyl ether was dissolved in deuterated methanol-d_3 and NMR spectrum taken. The solvent was evaporated, 2,7-diamino-9-fluorenyl phenyl ether photolyzed in water and organic layer extracted with dichloromethane(DCM). DCM was evaporated and NMR spectrum of photolyzed mixture taken again in deuterated methanol-d_3. However, due to many identified peaks on the spectrum and poor solubility, the results were inconclusive.

The released phenol could have not been detected by spot test either due to the presence of amino functions.

4.3.2. Discussion

Experiencing similar problems as in the case of acetate derivative, we could not quantatively determine the rate of release of the phenol from this system. We assume that phenol is released based on the UV-VIS spectrum of the photolyzed compound in basic solution, however we suspect that the quantum yield of the phenol release in this case is low suggesting that poor leaving groups should not be caged by this phototrigger.

5. Conclusions

Our studies on 2,7-diamino-9-fluorenol showed that introducing two amino groups positions 2 and 7 of the parent compound shifts the absorption of the chromophore towards the visible area. The solubility in aqueous solutions is also improved. The lifetimes of the transient intermediates in TFE and HFIP are prolonged. However, higher efficiency of the reaction, as expected based on the Zimmerman's effect, has not been proved.

2,7-diamino-9-fluorenol upon photolysis in polyfluorinated alcohols exibits an interesting behavior of forming transient intermediates in the infrared area. For the time being, despite lots of efforts, only few conclusions have been made and their character is still unclear. We suspect their cationic character, formed either via singlet or a very fast triplet state. Photolyse of 2,7-diamino-9-fluorenol in methanol and water are in agreement with what was expected.

2,7-diamino-9-fluorenyl acetate is potentially a good system for releasing acetic acid though quantum yield of the release is still not measured due to practical difficulties encountered.

2,7-Diamino-9-fluorenyl phenyl ether liberates phenol with disappointingly low efficiency, illustrating that poor leaving groups cannot be efficiently released by this phototrigger.

6. Experimental

6.1. Irradiation

Solutions were irradiated in a quartz UV-cell with a Hanau medium pressure mercury lamp. Its stability after burning for 30 minutes was ± 2%, as checked with a photodiode. Band-pass filters were used to isolate the desired line. The solution concentrations were ~ 10^{-3} M and were stirred with a magnetic stirrer during the irradiation in order to achieve equal exposure to the light. Absorption spectra were recorded on a Perkin Elmer Lambda 19 spectrometer.

6.2. Flash photolysis

The measurements were carried out exciting the sample in a cuvette of 4.5 cm path length and 1 cm wide with the standard nanosecond laser flash photolysis (LFP) setup in our lab for transients on time scales from 30 ns to 100 μs. A Lambda Physik Compex 205 excimer laser (pulse width <20ns, pulse energy <200mJ) operated at 351 nm (XeF) and at 308 nm (XeCl), and a pulsed Xenon arc (Osram XBO 250 W) as the monitoring beam, were utilized.

The detection system allowed monitoring the kinetics at single wavelengths using a transient digitizer or the whole transient spectrum at a given time delay, in digital form with nanosecond resolution, using an Optical Multichannel Analyzer. Kinetic and spectrographic data were processed and analyzed by computer. Analyses of transient decays were performed using the nonlinear fitting program MacFitFlash version 2.0.1 non-FPU for the Power Macintosh. Spectrographic data have been recorded with CCD camera and analyzed by Andor *i* Star software. Absorption spectra were recorded on a HP diode array spectrophotometer. The setup has been described previously in detail elsewhere[71]. Solutions were degassed by three freeze-pump-thaw cycles.

All measurements have been performed in air-saturated solutions, if not specified otherwise. Care was also taken to minimize exposure of the samples to the monitoring light by using

light shutters and appropriate filters. SPECFIT 32 and Origin 7.0 were used for global analysis and kinetics fitting respectively.

6.3. Analytical equipment

NMR spectroscopy: Bruker 400 MHz spectrometer was used for recording NMR spectra. ^{1}H and ^{13}C NMR data were measured in DMF in the case of 2,7-diamino-9-fluorenol and in DMSO in the case of its derivatives. The chemical shifts are expressed in parts per million using tetramethylsilane (TMS) as an internal standard (^{1}H data). Coupling constants are given in Hz. ChemDraw Ultra, version 6.0, software was used to assist the assignment of carbon atoms (^{13}C data).

Gas-Chromatography-Mass Spectroscopy: Samples for GC/MS analysis were dissolved in acetone or water (approx. 1% by mass) and were analyzed on a Hewlett Packard Series II gas chromatograph coupled with mass selective detector HP 5971 Series. Two types of columns were used: a) 25 m Dimethylsilicone (OV-1, OV-101, SE-30) or b) 25 m, phenyl-methylsilicon (OV-3, SE-52). Valves were set to ca. 1 ml/min flow and 20:1 split.

Mass Spectroscopy: Mass spectrometers VG70-250 and Finnigan MAT 312 were used. Mass spectra were carried out by Dr. H. Nadig at the Institute for Organic Chemistry at the University of Basel. The ion generation was achieved by electron impact (EI) or bombardment with fast xenon atoms (FAB). Nitrobenzyl alcohol was used as a matrix and sodium chloride as an additive. The data are given in mass units per charge (m/z).

UV-Visible spectroscopy: UV spectra were obtained on a Agilent 8453 and Perkin-Elmer Lambda 9 UV-Vis spectrophotometers. The solutions were measured in a quartz UV-cell and the concentrations were ~ 10^{-5} M.

Fluorescence spectroscopy: Fluorescence spectra were taken on a Spex Fluorolog instrument, model 111C, using 150 W, cw Xenon lamp as a source.

pH Titrations: Titrations were run under N_2 atmosphere at 25 ± 0.1 °C and using combined glass electrode (8M HCl) on the automatic titrator previously described[72], consisting of a Metrohm 605 pH-meter, a Metrohm 665 burette, a thermostatted titration vessel and 286-AT PC controlling the set up. A computer program TITFIT was used for numerical treatment of potentiometric data by using analytical derivatives and optimizing subroutines with the Newton-Gauss-Marquardt algorithm, described in detail elsewhere[73]. pH titrations were carried out by Ms. L. Siegfried at the Institute for Inorganic Chemistry at the University of Basel.

Melting points apparatus: Electrothermal Model 1A-8101 digital capillary melting point apparatus was used for determining the melting points and they are uncorrected.

Calculations: The primary goal of these theoretical investigations was to support or exclude conceivable reaction mechanisms and to predict some of the characteristics of the given transients. PPP SCF CI and TD DFT calculations have been carried out in order to predict the wavelengths and probabilities for the transients to occur. Calculations of the radical cation of the 2,7-diamino-9-fluorenol have been done. Geometry was optimized according to either B3LYP density functional theory or MP2 perturbation theory with the 6-31G(d) basis set. Excited states were computed using Configuration Interaction approach (CI-Singles). All the calculations were carried out using GAUSSIAN 03 package.

Telsonic Ultrasonics TPC-15 ultrasonic was used for mixing the solutions.

Rotavapor Büchi R 200 with a Büchi B-490 water bath was utilized for evaporation of the reaction mixtures, and *Vacuumbrand* Diaphragm vacuum pump Type MZ 2 for drying the compounds.

6.4. Materials

Synthesis:

2,7-dinitro-fluorenone, 97% purity, and 9-fluorenol, 96% purity, were obtained from Aldrich and used as received. A suspension of Raney Nickel ready to use was purchased from Fluka. A hydrazine hydrate 85% solution was obtained from Riedel-de Haën Fine Chemicals, whereas the 100% one was purchased from Aldrich. Silver oxide (≥ 99.0%), acetic anhydride (>99%), phenol, (puriss, p.a.≥ 99.5%), glacial acetic acid (≥ 99.0%), tetrahydrofuran (technical), perchloric acid (60%, p.a.), aniline (purum, ≥ 99.0% (GC)) and ethanol (pure, absolute) were all purchased from Fluka and used as received. Copper (I) iodide was obtained from Merck. 1,10-phenanthroline monohydrate puriss.; p.a.; ≥ 99.0% (HPLC) and potassium fluoride on aluminium oxide, ~ 5.5 mmol F^- /g, were obtained from Fluka. Acetonitrile used for synthesis was of ≥ 99.5% (GC) quality, puriss.; absolute; over molecular sieve (≤0.01% water) and obtained from Fluka. Phenyl iodide puriss.; ≥ 99% (GC) and cobaltous chloride anhydrous purum p.a.; ≥ 98.0% (KT) were purchased from Fluka.

Phosphorus pentoxide pure, >97%, was obtained from Fluka. Argon used for synthesis was of 4.6 qualities and purchased from Linde.

Measurements:

1,1,1,3,3,3-Hexafluoroisopropyl alcohol (HFIP) and 2,2,2-trifluoroethanol (TFE) were purchased from Fluka AG, purity ≥99.0% (GC), and used as received. Acetonitrile was obtained from Fluka AG, HPLC grade. Acetone was purchased from Schweizerhall Chemie AG, chemically pure. Di-*tert*-butyl peroxide (DTBP), 98% purity, was obtained from Aldrich. Sodium hydroxide was prepared in the lab as 10% aqueous solution (pH = 14). Doubly distilled water was used to prepare aqueous solutions as well as the nucleophile for accelerating transient decay.

Chloroform-d_3, 99.95% purity, was purchased from Uetikon. *N,N*-Dimethyl formamide-d_7 (DMF-d_7) was of 99.5% purity and purchased from Armar. Dimethyl sulfoxide-d_6 (*DMSO*-d_6), 99.98% purity, was obtained from Cambridge Iso. Lab. Acetonitrile-d_3, 99 atom % D, was purchased from Acros Organics.

7. References

1. Greene, T. W. & Wuts, P. G. M. *Protective Groups in Organic Synthesis. 3rd Ed* (New York, 1999).
2. Pillai, V. N. R. Photoremovable protecting groups in organic synthesis. *Synthesis*, 1-26 (1980).
3. Merrifield, R. B., Barany, G., Cosand, W. L., Engelhard, M. & Mojsov, S. 488-502 (1977).
4. Bochet, C. G. Photolabile protecting groups and linkers. *Journal of the Chemical Society, Perkin Transactions 1*, 125-142 (2002).
5. Pillai, V. N. R. *Organic Photochemistry* **9**, 225 (1987).
6. Adams, S. R. & Tsien, R. Y. Controlling cell chemistry with caged compounds. *Annu Rev Physiol FIELD Full Journal Title:Annual review of physiology* **55**, 755-784. (1993).
7. McCray, J. A. & Trentham, D. R. Properties and uses of photoreactive caged compounds. *Annual Review of Biophysics and Biophysical Chemistry* **18**, 239-270 (1989).
8. Pelliccioli Anna, P. & Wirz, J. Photoremovable protecting groups: reaction mechanisms and applications. *Photochem Photobiol Sci FIELD Full Journal Title:Photochemical & photobiological sciences : Official journal of the European Photochemistry Association and the European Society for Photobiology* **1**, 441-458. (2002).
9. Marriott, G. *Caged Compounds. [In: Methods Enzymol., 1998; 291]* (1998).
10. Morrison, H. & Editor. *Biological Applications of Photochemical Switches. [In: Bioorg. Photochem., 1993; 2]* (1993).
11. Falvey, D. E. Dynamic Studies in Biology: Phototriggers, Photoswitches, and Caged Biomolecules edited by Maurice Goeldner and Richard Givens. *Journal of the American Chemical Society* **127**, 16747 (2005).
12. Kaplan, J. H., Forbush, B., III & Hoffman, J. F. Rapid photolytic release of adenosine 5'-triphosphate from a protected analog: utilization by the sodium:potassium pump of human red blood cell ghosts. *Biochemistry* **17**, 1929-1935 (1978).

13. Il'ichev Yuri, V., Schworer Markus, A. & Wirz, J. Photochemical reaction mechanisms of 2-nitrobenzyl compounds: methyl ethers and caged ATP. *J Am Chem Soc FIELD Full Journal Title:Journal of the American Chemical Society* **126**, 4581-4595. (2004).
14. Rajesh, C. S., Givens, R. S. & Wirz, J. Kinetics and Mechanism of Phosphate Photorelease from Benzoin Diethyl Phosphate: Evidence for Adiabatic Fission to an a-Keto Cation in the Triplet State. *Journal of the American Chemical Society* **122**, 611-618 (2000).
15. Givens, R. S. & Park, C.-H. Hydroxyphenacyl ATP: a new phototrigger. V. *Tetrahedron Letters* **37**, 6259-6262 (1996).
16. Park, C.-H. & Givens, R. S. New Photoactivated Protecting Groups. 6. p-Hydroxyphenacyl: A Phototrigger for Chemical and Biochemical Probes. *Journal of the American Chemical Society* **119**, 2453-2463 (1997).
17. Givens, R. S. *et al.* New Phototriggers 9: p-Hydroxyphenacyl as a C-Terminal Photoremovable Protecting Group for Oligopeptides. *Journal of the American Chemical Society* **122**, 2687-2697 (2000).
18. Du, X., Frei, H. & Kim, S. H. Comparison of nitrophenylethyl and hydroxyphenacyl caging groups. *Biopolymers FIELD Full Journal Title:Biopolymers* **62**, 147-149. (2001).
19. Kandler, K., Katz, L. C. & Kauer, J. A. Focal photolysis of caged glutamate produces long-term depression of hippocampal glutamate receptors. *Nature Neuroscience* **1**, 119-123 (1998).
20. Conrad, P. G., II *et al.* p-Hydroxyphenacyl Phototriggers: The Reactive Excited State of Phosphate Photorelease. *Journal of the American Chemical Society* **122**, 9346-9347 (2000).
21. Conrad, P. G., 2nd, Givens, R. S., Weber, J. F. & Kandler, K. New phototriggers: extending the p-hydroxyphenacyl pi-pi absorption range. *Org Lett FIELD Full Journal Title:Organic letters* **2**, 1545-1547. (2000).
22. Schade, B. *et al.* Deactivation Behavior and Excited-State Properties of (Coumarin-4-yl)methyl Derivatives. 1. Photocleavage of (7-Methoxycoumarin-4-yl)methyl-Caged Acids with Fluorescence Enhancement. *Journal of Organic Chemistry* **64**, 9109-9117 (1999).

23. Eckardt, T. *et al.* Deactivation behavior and excited-state properties of (coumarin-4-yl)methyl derivatives. 2. Photocleavage of selected (coumarin-4-yl)methyl-caged adenosine cyclic 3',5'-monophosphates with fluorescence enhancement. *J Org Chem FIELD Full Journal Title:The Journal of organic chemistry* **67**, 703-710. (2002).
24. Schonleber, R. O., Bendig, J., Hagen, V. & Giese, B. Rapid photolytic release of cytidine 5'-diphosphate from a coumarin derivative: a new tool for the investigation of ribonucleotide reductases. *Bioorganic & Medicinal Chemistry* **10**, 97-101 (2001).
25. Furuta, T., Torigai, H., Sugimoto, M. & Iwamura, M. Photochemical Properties of New Photolabile cAMP Derivatives in a Physiological Saline Solution. *Journal of Organic Chemistry* **60**, 3953-3956 (1995).
26. Furuta, T. *et al.* Brominated 7-hydroxycoumarin-4-ylmethyls: photolabile protecting groups with biologically useful cross-sections for two photon photolysis. *Proceedings of the National Academy of Sciences of the United States of America* **96**, 1193-1200 (1999).
27. Atemnkeng Walters, N., Louisiana, I. I. L. D., Yong Promise, K., Vottero, B. & Banerjee, A. 1-[2-(2-hydroxyalkyl)phenyl]ethanone: a new photoremovable protecting group for carboxylic acids. *Org Lett FIELD Full Journal Title:Organic letters* **5**, 4469-4471. (2003).
28. Coleman, M. P. & Boyd, M. K. S-Pixyl Analogues as Photocleavable Protecting Groups for Nucleosides. *Journal of Organic Chemistry* **67**, 7641-7648 (2002).
29. Fedoryak, O. D. & Dore, T. M. Brominated Hydroxyquinoline as a Photolabile Protecting Group with Sensitivity to Multiphoton Excitation. *Organic Letters* **4**, 3419-3422 (2002).
30. Zhu, Y., Pavlos, C. M., Toscano, J. P. & Dore, T. M. 8-Bromo-7-hydroxyquinoline as a Photoremovable Protecting Group for Physiological Use: Mechanism and Scope. *Journal of the American Chemical Society* **128**, 4267-4276 (2006).
31. Corrie, J. E. T. & Trentham, D. R. Caged nucleotides and neurotransmitters. *Bioorganic Photochemistry* **2**, 243-305, 241plate (1993).
32. Gee, K. R., Carpenter, B. K. & Hess, G. P. Synthesis, photochemistry, and biological characterization of photolabile protecting groups for carboxylic acids and neurotransmitters. *Methods in Enzymology* **291**, 30-50 (1998).

33. Kaupp, U. B. *et al.* The signal flow and motor response controlling chemotaxis of sea urchin sperm. *Nature Cell Biology* **5**, 109-117 (2003).
34. Walker, J. W. *et al.* Signaling pathways underlying eosinophil cell motility revealed by using caged peptides. *Proceedings of the National Academy of Sciences of the United States of America* **95**, 1568-1573 (1998).
35. Tatsu, Y., Shigeri, Y., Sogabe, S., Yumoto, N. & Yoshikawa, S. Solid-phase synthesis of caged peptides using tyrosine modified with a photocleavable protecting group: application to the synthesis of caged neuropeptide Y. *Biochemical and Biophysical Research Communications* **227**, 688-693 (1996).
36. Dussy, A. *et al.* New light-sensitive nucleosides for caged DNA strand breaks. *ChemBioChem* **3**, 54-60 (2002).
37. Theriot, J. A., Mitchison, T. J., Tilney, L. G. & Portnoy, D. A. The rate of actin-based motility of intracellular Listeria monocytogenes equals the rate of actin polymerization. *Nature (London, United Kingdom)* **357**, 257-260 (1992).
38. Vincent, J. P. & O'Farrell, P. H. The state of engrailed expression is not clonally transmitted during early Drosophila development. *Cell (Cambridge, MA, United States)* **68**, 923-931 (1992).
39. Denk, W., Strickler, J. H. & Webb, W. W. Two-photon laser scanning fluorescence microscopy. *Science (Washington, DC, United States)* **248**, 73-76 (1990).
40. Brown, E. B. & Webb, W. W. Two-photon activation of caged calcium with submicron, submillisecond resolution. *Methods Enzymol FIELD Full Journal Title:Methods in enzymology* **291**, 356-380. (1998).
41. Brown, E. B., Shear, J. B., Adams, S. R., Tsien, R. Y. & Webb, W. W. Photolysis of caged calcium in femtoliter volumes using two-photon excitation. *Biophysical Journal* **76**, 489-499 (1999).
42. Kiskin, N. I., Chillingworth, R., McCray, J. A., Piston, D. & Ogden, D. The efficiency of two-photon photolysis of a \"caged\" fluorophore, o-1-(2-nitrophenyl)ethylpyranine, in relation to photodamage of synaptic terminals. *European Biophysics Journal* **30**, 588-604 (2002).
43. Hopt, A. & Neher, E. Highly nonlinear photodamage in two-photon fluorescence microscopy. *Biophysical Journal* **80**, 2029-2036 (2001).

44. Lipp, P. & Niggli, E. Fundamental calcium release events revealed by two-photon excitation photolysis of caged calcium in guinea-pig cardiac myocytes. *Journal of Physiology (Cambridge, United Kingdom)* **508**, 801-809 (1998).

45. Wan, P. & Krogh, E. Evidence for the generation of aromatic cationic systems in the excited state. Photochemical solvolysis of fluoren-9-ol. *Journal of the Chemical Society, Chemical Communications*, 1207-1208 (1985).

46. Wan, P. & Krogh, E. Contrasting photosolvolytic reactivities of 9-fluorenol vs. 5-suberenol derivatives. Enhanced rate of formation of cyclically conjugated four p carbocations in the excited state. *Journal of the American Chemical Society* **111**, 4887-4895 (1989).

47. Wan, P., Krogh, E. & Chak, B. Enhanced formation of 8p(4n) conjugated cyclic carbanions in the excited state: first example of photochemical C-H bond heterolysis in photoexcited suberene. *Journal of the American Chemical Society* **110**, 4073-4074 (1988).

48. McClelland, R. A., Cozens, F. L., Li, J. & Steenken, S. Flash photolysis study of a Friedel-Crafts alkylation. Reaction of the photogenerated 9-fluorenyl cation with aromatic compounds. *Journal of the Chemical Society, Perkin Transactions 2: Physical Organic Chemistry*, 1531-1543 (1996).

49. Mecklenburg, S. L. & Hilinski, E. F. Picosecond spectroscopic characterization of the 9-fluorenyl cation in solution. *Journal of the American Chemical Society* **111**, 5471-5472 (1989).

50. McClelland, R. A., Mathivanan, N. & Steenken, S. Laser flash photolysis of 9-fluorenol. Production and reactivities of the 9-fluorenol radical cation and the 9-fluorenyl cation. *Journal of the American Chemical Society* **112**, 4857-4861 (1990).

51. Gaillard, E., Fox, M. A. & Wan, P. A kinetic study of the photosolvolysis of 9-fluorenol. *Journal of the American Chemical Society* **111**, 2180-2186 (1989).

52. McClelland, R. A. Flash photolysis generation and reactivities of carbenium ions and nitrenium ions. *Tetrahedron* **52**, 6823-6858 (1996).

53. Gurzadyan, G. G. & Steenken, S. Solvent-dependent C-OH homolysis and heterolysis in electronically excited 9-fluorenol: the life and solvation time of the 9-fluorenyl cation in water. *Chemistry--A European Journal* **7**, 1808-1815 (2001).

54. Matesich, M. A., Knoefel, J., Feldman, H. & Evans, D. F. Transport properties in hydrogen bonding solvents. VII. Conductance of electrolytes in 1,1,1,3,3,3-hexafluoro-2-propanol. *Journal of Physical Chemistry* **77**, 366-369 (1973).

55. Peng, L., Silman, I., Sussman, J. & Goeldner, M. Biochemical evaluation of photolabile precursors of choline and of carbamylcholine for potential time-resolved crystallographic studies on cholinesterases. *Biochemistry* **35**, 10854-10861 (1996).

56. Loudwig, S. & Goeldner, M. N-Methyl-N-(o-nitrophenyl)carbamates as photolabile alcohol protecting groups. *Tetrahedron Letters* **42**, 7957-7959 (2001).

57. Pirrung, M. C. & Bradley, J.-C. Dimethoxybenzoin Carbonates: Photochemically-Removable Alcohol Protecting Groups Suitable for Phosphoramidite-Based DNA Synthesis. *Journal of Organic Chemistry* **60**, 1116-1117 (1995).

58. Zehavi, U., Amit, B. & Patchornik, A. Light-sensitive glycosides. I. 6-Nitroveratryl b-D-glucopyranoside and 2-nitrobenzyl b-D-glucopyranoside. *Journal of Organic Chemistry* **37**, 2281-2285 (1972).

59. Nicolaou, K. C., Winssinger, N., Pastor, J. & DeRoose, F. A General and Highly Efficient Solid Phase Synthesis of Oligosaccharides. Total Synthesis of a Heptasaccharide Phytoalexin Elicitor (HPE). *Journal of the American Chemical Society* **119**, 449-450 (1997).

60. Specht, A. & Goeldner, M. 1-(o-Nitrophenyl)-2,2,2-trifluoroethyl ether derivatives as stable and efficient photoremovable alcohol-protecting groups. *Angewandte Chemie, International Edition* **43**, 2008-2012 (2004).

61. Jobron, L. & Hindsgaul, O. Novel Para-Substituted Benzyl Ethers for Hydroxyl Group Protection. *Journal of the American Chemical Society* **121**, 5835-5836 (1999).

62. Plante, O. J., Buchwald, S. L. & Seeberger, P. H. Halobenzyl Ethers as Protecting Groups for Organic Synthesis. *Journal of the American Chemical Society* **122**, 7148-7149 (2000).

63. Fukase, K., Tanaka, H., Torii, S. & Kusumoto, S. 4-Nitrobenzyl group for protection of hydroxyl functions. *Tetrahedron Letters* **31**, 389-392 (1990).

64. Balcom, D. & Furst, A. Reductions with hydrazine hydrate catalyzed by Raney nickel. I. Aromatic nitro compounds to amines. *Journal of the American Chemical Society* **75**, 4334 (1953).

65. Pan, H.-L. & Fletcher, T. L. Derivatives of fluorene. 35. Hydrazine-hydrate and Raney-nickel reduction of nitrofluorenones to aminofluoren-9-ols. *Synthesis*, 192-194 (1972).
66. Fieser, L. F. & Fieser, M. *Reagents for Organic Synthesis* (1967).
67. Hosseinzadeh, R., Tajbakhsh, M., Mohadjerani, M. & Alikarami, M. Copper-catalyzed etherification of aryl iodides using KF/Al2O3. An improved protocol. *Synlett*, 1101-1104 (2005).
68. Ahmad, S. & Iqbal, J. A new acylation catalyst. *Journal of the Chemical Society, Chemical Communications*, 114-115 (1987).
69. Guzik, F. F. & Colter, A. K. Substituent effects in the fluorene series. I. Synthesis and acetolysis of some dinitro-9-fluorenyl p-toluenesulfonates. *Canadian Journal of Chemistry* **43**, 1441-1447 (1965).
70. Steven L. Murov, I. C., Gordon L. Hug (ed.) *Handbook of Photochemistry, 2nd edition* (1993).
71. Leyva, E., Platz, M. S., Persy, G. & Wirz, J. Photochemistry of phenyl azide: the role of singlet and triplet phenylnitrene as transient intermediates. *Journal of the American Chemical Society* **108**, 3783-3790 (1986).
72. Gampp, H., Maeder, M., Zuberbuehler, A. D. & Kaden, T. A. Microprocessor-controlled system for automatic acquisition of potentiometric data and their nonlinear least-squares fit in equilibrium studies. *Talanta* **27**, 513-518 (1980).
73. Zuberbuehler, A. D. & Kaden, T. A. TITFIT, a comprehensive program for numerical treatment of potentiometric data by using analytical derivatives and automatically optimized subroutines with the Newton-Gauss-Marquardt algorithm. *Talanta* **29**, 201-206 (1982).

8. Summary

The main goal of this work was that of identifying new photochemical systems that could be applied in the design of novel photoremovable protecting groups. In particular, we looked for a system that would efficiently release alcohol, as this could be readily applied in biology. The idea was based on the photochemistry of 9-fluorenol which is well established and known. Efforts were undertaken to enhance the desired properties of this system in order to be more biocompatible.

Our work showed that introducing two amino groups in positions 2 and 7 shifts the absorption of the chromophore towards the visible area of the spectrum, which is far less harmful to the biological environment than the UV light usually required for the deprotection of the ppg. The solubility in buffered aqueous solution was improved. We also expected, based on Zimmerman's "meta-ortho effect", that the substitution in meta-position would make the reaction more efficient, but our experiments did not allow us to prove this.
2,7-diamino-9-fluorenol was efficiently synthesized by reducing the corresponding commercially available dinitro ketone. Flash photolysis investigations were carried out to clarify the reaction mechanism in different solvents. Transients in the infrared area were observed in the solvents TFE and HFIP but their character remains unclear. We suspect their cationic character, and their formation either via singlet or a very fast triplet state. Our mechanistic studies provided rate constants of formation and decay of the transients in three different solvents (TFE, methanol and water).

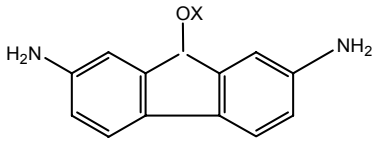

Two derivatives of 2,7-diamino-9-fluorenol (X = C_6H_5 and $COCH_3$) were synthesized using a four-step synthetic route based on the sequence ketone → hydrazone → diazo compound → ether/acetate. Subsequent reduction of the nitro derivatives so obtained yielded

the desired compounds in good yields. The idea was to study the quantum yield of formation of 2,7-diamino-9-fluorenol upon photolysis in water. The photorelease of these derivatives was elucidated by employing irradiation experiments and product analysis.

Despite problems encountered in analyzing the photolyzed mixtures, the results indicate that 2,7-diamino-9-fluorenyl acetate liberates acetic acid efficiently. The quantum yield of the release is yet to be determined.

Less satisfactory results were obtained when investigating the phenyl ether derivative, which proved to be poorly reactive. Preliminary investigations on the photochemistry of 2,7-diamino-9-fluorenyl phenyl ether in aqueous solution led us to conclude that phenol is released. However, the efficiency rate of release is very low and could not be quantitatively determined, suggesting that poor leaving groups should not be caged by this phototrigger.

9. Curriculum Vitae

Personal Data

Name	Dragana Zivkovic
Date of birth	March 11, 1977
Nationality	Serbian

Education and research experience

April 2007	PhD Degree under supervision of Prof. Dr. J.Wirz, University of Basel
Aug. 2002	Start of PhD studies, University of Basel
Jan.-June 2002	Traineeship in „Novartis“, Basel, Switzerland –working in Organic Lab CHAD
Oct. 1996-Oct. 2001	Chemistry study, University of Belgrade, Serbia
Sep. 1992-Jun. 1996	Grammar School, Gimnazija, Pirot, Serbia
Sep. 1984-Jun. 1992	Primary School, Osnovna Skola Sveti Sava, Pirot, Serbia

During my studies at University of Basel I attended lectures by:

E. Constable, M. Meuwly, A. Vedani, J. Wirz

10. Appendix

During my PhD study I have been involved in other projects, one of them measuring energy transfer of some compounds on water ices. For our study, we have been using bipotassium xanthone-2,7-disulfonate salt (XaSK2) and $EuCl_3$.

XaS^{2-} and Eu^{3+} are donor and acceptor with a large difference in charge thus a strong interaction, conceivably salt precipitation, would be expected. If they are in contact (XaEu) the energy transfer process will occur and is expected to be much faster in a frozen sample than in solution. The photoreactions were studied by nanosecond flash photolysis, in low-temperature water-ices, on different temperatures and varying the concentration of the samples.

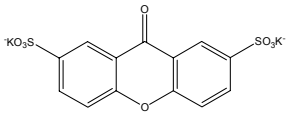

Xa

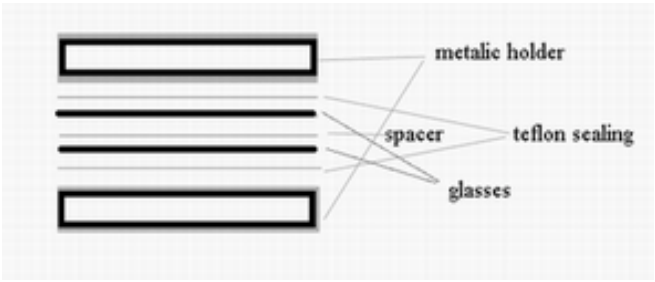

Scheme 1. The sample holder used for making the ice sample, sagittal intersection.

I also studied photochemical reaction mechanisms of benzocyclobutenyl diaziridine by trying to synthesize the compound (Scheme 2) and doing some laser flash photolysis experiments.

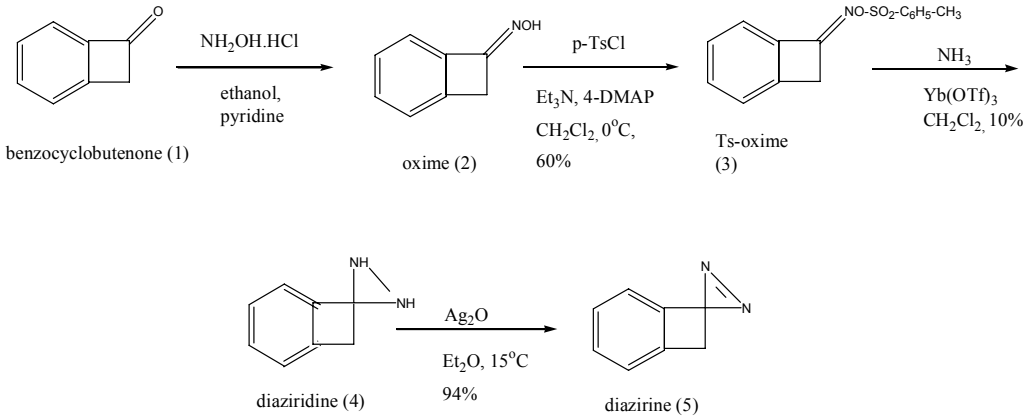

Scheme 2. Detailed synthesis scheme of benzocyclobutenyl diaziridine.

The calculations were performed to predict relative energies of reaction intermediates using Gaussian98. For B3LYP 6-31G* method no ZPI correction has been made.

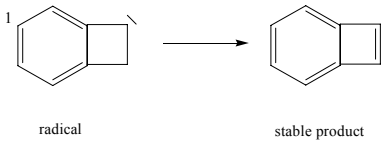

difference of E ZPE, kcal/mol	radical	transition state	stable product
B3LYP 6-31G*	38.505	68.518	0
G3 MP2	38.905	45.709	0

Table 1. Calculated relative energies of reaction intermediates. Theoretical values include ZPVEs from corresponding frequency calculations (not scaled).